Fakultät für Medizin

Neurologische Klinik und Poliklinik

White Matter Lesion Size and Gadolinium Accumulation: Two Important Aspects of Multiple Sclerosis Evaluation by Modern Magnetic Resonance Imaging

Sophia Grahl

Vollständiger Abdruck der von der Fakultät für Medizin der Technischen Universität München zur Erlangung des akademischen Grades eines

Doctor of Philosophy (Ph.D.)

genehmigten Dissertation.

Vorsitzende: Prof. Dr. Agnes Görlach

Betreuer: Prof. Dr. Mark Mühlau

Prüfer der Dissertation:

1. Prof. Dr. Markus Ploner

2. Priv.-Doz. Dr. Christian Sorg

Die Dissertation wurde am 02.10.2020 bei der Fakultät für Medizin der Technischen Universität München eingereicht und durch die Fakultät für Medizin am 03.12.2020 angenommen.

Contents

List of Tables

List of Figures

Abstract

Multiple sclerosis (MS) is the leading cause of non-traumatic disability in young adults. The auto-immune disease is characterized by inflamed regions within the brain and spinal cord. These so-called lesions are visible in-vivo in magnetic resonance imaging (MRI) scans and play a crucial role in diagnosing the disease and monitoring disease progression. This thesis investigates the question whether two aspects of common practice in the diagnostic workup of patients with suspected MS can still be regarded as reasonable.

We first aimed to provide an evidence-based rationale for a white matter (WM) lesion size threshold in patients with relapsing-remitting MS (RRMS) in times of high-resolution MRI. We analyzed MRI scans from two different cohorts, each comprising patients with RRMS and control subjects (CS), obtained at scanners from two different vendors. Both cohorts were examined with fluid-attenuated inversion recovery and T1-weighted (T1w) sequences. In total, we studied 232 patients with RRMS (Expanded Disability Status Scale: mean = 1.6 +/- 1.2; age: mean = 36 years +/- 10 years) as well as 116 age- and sex-matched CS. We calculated odds ratios of WM lesion volumes. The WM lesion size threshold, which discriminated best between patients and CS, was estimated with receiver operating characteristic curve analysis. In both cohorts, odds ratios increased continuously with increasing WM lesion volumes, and discriminative power was highest at a WM lesion size threshold of 3 millimeter in diameter. Hence, the WM lesion size threshold of 3 millimeter in diameter, as stipulated in the current diagnostic criteria of MS (Thompson et al., 2018b), seems a reasonable choice for three-dimensional MRI sequences at 3 Tesla.

In a second project we investigated, if repetitive application of gadolinium-based contrast agents (GBCA) changes signal intensity in unenhanced T1w images and how chelate types (linear vs. cyclic) differ. Signal change would be a sign for

Gadolinium (Gd) deposition in the brain and potentially implicates the risk of unfavorable long-term effects. This issue is of special importance for patients with MS as monitoring disease course and therapy require regular follow-up MRI scans over many years. As activity of lesions is best discriminated by GBCA, MRI in MS patients often includes application of GBCA. We retrospectively analyzed 3233 unenhanced T1w images of 881 MS patients. After spatial normalization and intensity scaling, using a sphere within the pons, differences of all pairs of subsequent scans were calculated and, according to the first scan, attributed to either linear ($n = 2718$) or cyclic ($n = 385$) or no GBCA ($n = 130$). We performed regional analyses, focusing on the dentate nucleus (DN), and whole brain analyses. By one-sample t-tests, we searched for signal intensity increases within conditions; by two-sample t-tests, we compared conditions. Further we tested recent hypotheses on the reversibility of GBCA deposition. Regional analyses of the DN showed a significant increase only after administration of linear GBCA, even after a single GBCA administration. This increase differed significantly ($p < 0.001$) from the other conditions (cyclic and no GBCA). Whole brain analyses revealed T1w signal increases only after administration of linear GBCA within two regions, the DN and globus pallidus. Additional analyses did not indicate any decline of Gd deposition in the brain. Our data point towards Gd deposition in the brain after administration of linear GBCA even after a single administration.

The results of both projects justify current recommendations for the diagnostic workup of suspected MS. The traditional white matter lesion size threshold of 3 mm in diameter should still be respected. In patients with suspected MS, cyclic GBCA should not be withheld for the fear of possible toxic effects.

Zusammenfassung

Die Multiple Sklerose (MS) ist eine der wichtigsten Ursachen für nicht-traumatisch bedingte Behinderung bei jungen Erwachsenen. Die Autoimmunerkrankung zeichnet sich durch entzündliche Läsionen (Plaques) in Gehirn und Rückenmark aus. Läsionen lassen sich in-vivo mittels Magnetresonanztomografie (MRT)-Bildern nachweisen und spielen eine wichtige Rolle bei der Diagnose der Krankheit sowie ihrer Verlaufsbeurteilung. Die vorliegende Arbeit geht der Frage nach, inwieweit zwei übliche Vorgehensweisen im Rahmen des MRT gestützten Diagnoseprozesses weiterhin akzeptabel sind.

In diesem Zusammenhang untersucht das erste Projekt, inwiefern der bisher festgelegte kleinste Läsionsdurchmesser von 3 mm auch im Zeitalter hochauflösender MRT-Bilder valide ist. Es wurden MRT-Bilder zweier unterschiedlicher MR Geräte untersucht und dabei jeweils Bilder von Patienten mit schubförmig-remittierender MS (RRMS) mit Bildern von Kontrollprobanden verglichen. Von beiden Kohorten wurden 3-dimensionale Fluid-Attentuated Inversion Recovery und T1 gewichtete (T1w) MR Bilder analysiert, sodass insgesamt 232 RRMS Patienten und 116 Kontrollprobanden im gleichen Alter und Geschlechterverhältnis in die Studie eingeschlossen wurden. Wir haben Odds Ratios über Läsionsvolumen errechnet und eine Receiver Operating Curve Analyse durchgeführt, um diejenige minimale Läsionsgröße festzulegen, welche am besten zwischen MS Patienten und Kontrollen diskriminiert. In beiden Kohorten wurden kontinuierlich steigende Odds Ratios mit zunehmendem Läsionsvolumen beobachtet. Die beste Diskriminierung wurde für ein Läsionsvolumen von 0.015 ml gefunden, welches einem Durchmesser von 3 mm entspricht.

In einem zweiten Projekt wurde untersucht, ob die wiederholte Verwendung von Gadolinium-haltigem Kontrastmittel (GBCA) zu Signalintensitätsveränderungen im

Gehirn von MS Patienten führt und inwiefern sich diese Veränderung zwischen GBCA-Formen unterscheidet. Da MS Patienten im Laufe ihrer Krankheitsgeschichte häufig und über mehrere Jahre hinweg GBCA erhalten, können sie als besondere Risikogruppe für mögliche Langzeitschäden durch Gadoliniumablagerungen im Gehirn betrachtet werden. Es wurden 3233 native T1w MRT Bilder von insgesamt 881 MS Patienten retrospektiv untersucht. Nach räumlicher Normalisierung und Signalintensitätsskalierung der MRT Bilder wurden Differenzbilder errechnet und einer Gruppe zugeordnet, je nach Art des verabreichten GBCA am jeweils ersten Zeitpunkt. Durch dieses Vorgehen ergab sich eine Gruppenstärke von 2718 Bildern in der linearen GBCA Gruppe, 385 in der zyklischen GBCA Gruppe und 130 in der Gruppe ohne vorherige GBCA Gabe. Analysen wurden mit Fokus auf den Nucleus dentatus und über das gesamte Gehirn durchgeführt. Einstichproben T-Tests wurden verwendet, um Signalveränderungen innerhalb einer Gruppe zu untersuchen. Mit Hilfe von T-Tests für 2 Stichproben wurden die Gruppen miteinander verglichen. Zusätzlich wurden Untergruppen gebildet, um die Reversibilität der Signalveränderungen zu prüfen. Die Analysen deuten auf eine Signalveränderung im Nucleus dentatus lediglich nach Gabe linearer GBCA hin, nicht aber nach zyklischen GBCA. Analysen über das gesamte Gehirn zeigen zusätzlich eine Signalveränderung nach linearem GBCA im Globus pallidus, nicht jedoch nach Gabe zyklischer GBCA. Außerdem fand sich kein Rückgang der Signalveränderungen nach der GBCA Gabe im längerfristigen Verlauf. Diese Ergebnisse legen nahe, dass es zu einer Gadolinium-Ablagerung im Gehirn bereits nach einer einzigen Gabe eines linearen GBCA kommt.

Zusammenfassend stützen beide Projekte die derzeitige klinische Praxis bei der diagnostischen Aufarbeitung von Patienten mit Verdacht auf MS in zweierlei Hinsicht. An der traditionellen Mindestläsionsgröße von 3 mm im Durchmesser sollte festgehalten werden. Die Gabe eines zyklischen GBCA erscheint nach wie vor vertretbar.

Abbreviations

BBB	blood brain barrier
CIS	clinically isolated syndrome
CNS	central nervous system
CS	control subject
CSF	cerebrospinal fluid
D	diameter
DIS	dissemination in time
DIT	dissemination in space
DN	dentate nucleus
EBV	Epstein-Barr virus
EDSS	Expanded disability status scale
FLAIR	fluid-attenuated inverse recovery
GBCA	gadolinium-based contrast agent
Gd	gadolinium
GM	grey matter
GP	globus pallidum
MR	magnetic resonance
MRI	magnetic resonance imaging
MS	multiple sclerosis
OR	odds ratio
ROC	receiver operating curve
RRMS	relapsing-remitting multiple sclerosis
SPMS	secondary progressive multiple sclerosis
T	tesla
T1w	T1- weighted

T2w	T2- weighted
TE	echo time
TR	repetition time
WM	white matter

1 Introduction

1.1 General aspects of MS

The first attempt to define multiple sclerosis (MS) was done in 1868. Jean-Martin Charcot proposed his triad of typical symptoms for patients suffering from “la sclérose en plaques”: nystagmus, intention tremor and scanning speech (Pearce, 2005). More than 100 years later, the introduction of magnetic resonance imaging (MRI) changed the diagnosis of MS dramatically (Young et al., 1981). Today, MS is known as the most frequent chronic disease of the central nervous system (Gold et al., 2012) and the leading cause of non-traumatic disability in young adults in Europe and North America (Koch-Henriksen & Sørensen, 2010). Until today, MRI is the most important paraclinical tool for the diagnosis of this burdensome disease. Demyelinating inflamed lesions in the central nervous system (CNS) are the hallmark of MS. They can be detected in T2-weighted (T2w) MRI as hyperintense regions within the white matter (WM). Most patients suffer in early stages of the disease from erratic episodes (relapses) of neurological deficits (e.g. vision problems, numbness or muscle weakness) as a consequence of WM lesions resulting from acute inflammation (relapsing-remitting MS; RRMS). Sometimes symptoms are not completely recovered during remitting phases and remaining impairment could accumulate over time (Compston & Coles, 2008). The phase of RRMS is usually followed by a gradual accumulation of neurological deficits over time, independent of inflammatory relapses (secondary-progressive MS; SPMS).

In this chapter, background information about MS, including epidemiology and pathophysiology is presented. Further, the diagnostic process and possible treatment options are discussed. Finally, a more detailed insight into the role of MRI as a diagnostic tool for this disease is given, focusing on current challenges.

1.1.1 Epidemiology

Multiple sclerosis is one of the best characterized neurological diseases in terms of epidemiology. There is a striking unequal geographical distribution across the world (Koch-Henriksen & Sørensen, 2010). With a median prevalence of 33 per 100 000 persons, the number of people with MS is estimated at 2.3 million worldwide (Browne et al., 2014). This number is likely to be an underestimation, especially given the lack of information from large populations like China or India (Multiple Sclerosis International Federation, 2013; Thompson et al., 2018a). Global distribution of MS is inhomogeneous, generally increasing with increasing distance from the equator. The highest prevalence is reported in North America (140 per 100 000 inhabitants) and Europe (108 per 100 000 inhabitants) and lowest in Sub-Saharan Africa (2.1 per 100 000 inhabitants) and East Asia (2.2 per 100 000 inhabitants)(Multiple Sclerosis International Federation, 2013). Considerable variations within continents, depending on latitude, can be observed. For example, Sweden has the highest (189 per 100 000 inhabitants) prevalence within Europe and Albania the lowest (22 per 100 000 inhabitants).

Beside geographical associations with MS prevalence, studies reveal that twice as many women as men suffer from MS (Multiple Sclerosis International Federation, 2013). On average MS is diagnosed at the age of 30, although diagnosis is possible at any age. Compared to general population, life expectancy of MS patients is reduced by 7 to 14 years (Leray et al., 2016; Scalfari et al., 2013).

The analysis of epidemiological data represents an important step towards understanding the causes and environmental risk factors of MS. The pathogenesis of MS is currently assumed to be multifactorial (Compston & Coles, 2008; Koch-Henriksen & Sørensen, 2010; Leray et al., 2016). Different genetic and environmental risk factors are involved and will be described below.

Several environmental factors, such as Epstein-Barr virus (EBV) infection, Vitamin D deficiency, smoking, obesity or latitude have been proposed as risk factors for the development of MS (Compston & Coles, 2008). A recent umbrella review summarizes results from 44 meta-analyses on environmental risk factors (Belbasis et al., 2015). Only three of the investigated risk factors showed consistent and strong evidence of an association with MS: seropositivity to EBV antigen, infectious mononucleosis and smoking (Belbasis et al., 2015). In fact, the infection with EBV yielded the largest odds ratio (OR $>$ 4) and is the strongest known environmental risk factor for MS (Ascherio & Munger, 2007a), whereas EBV in turn is the main cause of infectious mononucleosis (Belbasis et al., 2015). However, there is no common understanding on how EBV and MS are related in detail. Higher vitamin D level is associated with lower risk of MS, possibly through regulatory effects on B and T-cells (Rolf et al., 2016). This can in part explain the higher incidence of MS observed in regions further from the equator and thus with less sunlight exposure. The effect of smoking on the development of MS is consistent, but modest. Explanations rank from effects of smoking on the immune system to demyelination due to smoking or disruption of the blood-brain barrier, but they all remain hypothetical (Ascherio & Munger, 2007b; Belbasis et al., 2015).

Family studies provide useful information for the discrimination of genetic and environmental influences on MS susceptibility. In general the risk to develop MS is 20 to 50-fold higher for first-degree relatives of MS patients than in the general population (Compston & Coles, 2008; Ebers et al., 2004). Studies have found concordance rates for monozygotic twins to be five times higher than for dizygotic twins (25% vs. 5%) (Mumford et al., 1994; Willer et al., 2003). Taken together, these results suggest genetic involvement for the development of MS. Since the first correlation of the human leukocyte antigen (HLA) from the major histocompatibility complex (MHC) with MS in the 1970s (Jersild et al., 1972), more than 201 non-HLA

polymorphisms were described to be associated with a predisposition of MS (International Multiple Sclerosis Genetics Consortium, 2019). Most of them are located in genes, regulating immunomodulatory functions, nevertheless, the so far identified loci can account for only about a quarter of reported heritability (Sawcer et al., 2014). Recently, genome-wide association studies have emphasized, besides genetic risk factors, the importance of epigenetic mechanisms of DNA methylation in the development of MS as the interface of genetic and environmental risk factors (Andlauer et al., 2016).

To sum up, the exact cause of MS is still unclear, most likely it is a complex interplay of environmental and genetic risk factors. EBV infection, vitamin D deficiency and smoking are the most well-established environmental contributors and genetic risk factors include 32 HLA- associated and 201 non-HLA polymorphisms.

1.1.2 Pathophysiology

MS is an autoimmune-mediated disease, with T-cells and B-cells playing the leading role in the pathogenesis (Compston & Coles, 2008; Disanto et al., 2012; Thompson et al., 2018a). For a long time, T-cells, especially CD4+ T helper cells, have been considered the main drivers of aberrant immune responses in MS (Disanto et al., 2012). This theory was supported by the fact that several genetic MHC variants are risk factors for MS (see 1.1.1). MHC is known to play a central role in the activation of T-cells, and consequently the induction of an adaptive immune response (Kasper & Shoemaker, 2010). Additionally, experimental autoimmune encephalomyelitis (the animal model of MS) was directly triggered by the injection of specific T-cells (Kasper & Shoemaker, 2010). In the past few years however, B-cells have shifted into the focus of MS pathogenesis research, although the appearance of oligoclonal bands (OCB) in the cerebrospinal fluid (CSF) of MS patients has been known for long. OCB are produced by activated B-cells within the CNS compartment and are used

as a diagnostic marker (Disanto et al., 2012; Frohman et al., 2006; Thompson et al., 2018b). Moreover, several clinical studies demonstrated efficacy of B-cell depleting agents (e.g. (Hauser et al., 2017; Kappos et al., 2011), suggesting a causal role of B-cells in the MS pathogenesis. It may be noted that many aspects of the MS pathogenesis are still unclear, e.g. why immune responses against the CNS are initiated first, maintained and becoming chronical later in MS patients. To date, it has not been possible to determine individual triggers of MS.

1.1.3 Clinical aspects of MS

The diagnosis of MS is mainly based on structural MRI, clinical symptoms, neurophysiological testing and CSF analysis. For putative MS patients, a structural MRI is highly recommended, since abnormal MRI findings are present in more than 80% of clinically isolated syndrome (CIS) patients, who later convert into clinically definite MS (Fisniku et al., 2008). MRI findings suggestive of MS are T2-hyperintense multifocal lesions in brain and spinal cord MRI (Bot et al., 2002; Fazekas et al., 1999). The most widely spread diagnostic criteria for MS are the McDonald criteria, which are described in more detail in section 1.2.2.

In general, typical MS symptoms originate from acute inflammation, resulting in WM lesions, during relapse phases (Compston & Coles, 2008). Acute unilateral optic neuritis and sensory symptoms are most common (Brownlee et al., 2017). Yet, virtually all symptoms resulting from damage in the CNS can appear. Besides, fatigue pain or balance problems are also symptoms of MS (Multiple Sclerosis International Federation, 2013). Clinical symptoms in MS patients are in general heterogenous, depending on the location and extent of inflammatory activity. The most widely used method to assess impairment and disability in MS is the Expanded Disability Status Scale (EDSS). EDSS scores are based on examination by a neurologist and rate impairment on different functional scales, such as tractus pyramidalis, sensory, visual

or cerebellar function (Kurtzke, 1983). The scale rates from 0 (no disability) to 10 (death due to MS).

In the past 20 years, treatment options for MS patients have changed dramatically. Owing to the variability of disease courses, comorbidities and individual risk factors, treatment decisions are complex and thus require guidelines for evidence-based clinical treatment recommendations (Montalban et al., 2018; Rae-Grant et al., 2018). Currently, more than 10 drugs with different modes of action and different efficacy are available (Reich et al., 2018). Still, all of them interact with inflammatory processes and are assumed to be most efficacious in the early stage of the disease. Hence, diagnosing MS early and reliably has become key for a successful treatment of MS.

Section 1.1 gave a short overview over epidemiological, pathophysiological and clinical aspects of MS. Several environmental and genetic factors have been identified: EBV infection, vitamin D and smoking show the strongest correlation to the risk for development of MS. MS is an autoimmune inflammatory disease involving a complex interplay of T- and B-cells. Clinical symptoms and MRI play the crucial role in diagnosing MS. The following section will focus on more detail on the role of MRI in MS as the main focus of this thesis.

1.2 Magnetic resonance imaging in MS

1.2.1 The role of magnetic resonance imaging in MS

Gold standard for the identification of pathological substrates are in principle, histological studies. In MS, however, histological studies are only performed either post-mortem (autopsy) or in atypical cases (biopsy) (Filippi et al., 2012). Those histological studies are useful as they contribute to the understanding of detailed

pathogenic mechanisms. Nevertheless, their results are merely a snapshot in their respective timeline and can hardly depict disease progression in MS.

MRI provides a non-invasive, reproducible, broadly available, but still sensitive approach to detect abnormalities in the brain and spinal cord. MRI is crucial for the diagnosis of MS, the monitoring of disease progression, evaluating paraclinical disease activity as well as effectiveness of disease-modifying therapies. By developing new techniques or sequences in research, MRI plays an important role in order to achieve a better understanding of the heterogenic pathological mechanisms (Filippi et al., 2019; Reich et al., 2018). MRI is the only technique which is able to examine the entire CNS and has been the key diagnostic test for MS since 2001 (McDonald et al., 2001). As MRI is an indirect measure, the following section will give insight into how MRI signal alterations and pathological findings correlate in MS patients.

White matter lesions

The most obvious hallmark of MS in an MR image are focal WM lesions, resulting from inflammation and demyelination (Filippi et al., 2019). On T2w or fluid-attenuated inversion recovery (FLAIR) images, lesions appear as areas of increased (hyperintense) MR signal (Figure 1a). T2w hyperintensity reflects general alterations in water content and thus is at first glance difficult to distinguish from pathological changes due to other diseases like microvascular ischemic changes (Ali & Buckle, 2009). It is essential to investigate additional lesion characteristics, such as morphology or location, to be able to distinguish typical MS lesions from nonspecific lesions. MS typical lesions are round or ovoid, whereas irregular areas of hyperintensity mostly result from several confluent lesions (mostly periventricular) (Filippi et al., 2012). WM lesions are mainly located in the corpus callosum, the juxtacortical grey-white matter junction, the periventricular region, the infratentorial brain region, and the spinal cord (Fazekas et al., 1999; Filippi et al., 2012; Neema et al., 2007). Corpus callosum lesions often touch the ependymal surface of the ventricle

in a very typical bulging manner, in sagittal view called Dawson`s fingers (Ali & Buckle, 2009) (Figure 1b). The prognostic values of T2w hyperintensities was subject of many studies. A 10-year follow-up study found that patients with a clinical episode compatible with CIS (e.g. myelitis or optic neuritis) but without any WM lesions converted to clinically definite MS only in 19% of the cases, whereas almost 90% of CIS patients with two or more lesions converted to MS (Brex et al., 2002). The presence of infratentorial and deep WM lesions in the first year of diagnosis seems to be a predictor for the conversion to SPMS in a long-term follow-up studies (Chung et al., 2020). Furthermore lesion volume and its change is also correlated with disability after 20 years (Fisniku et al., 2008).

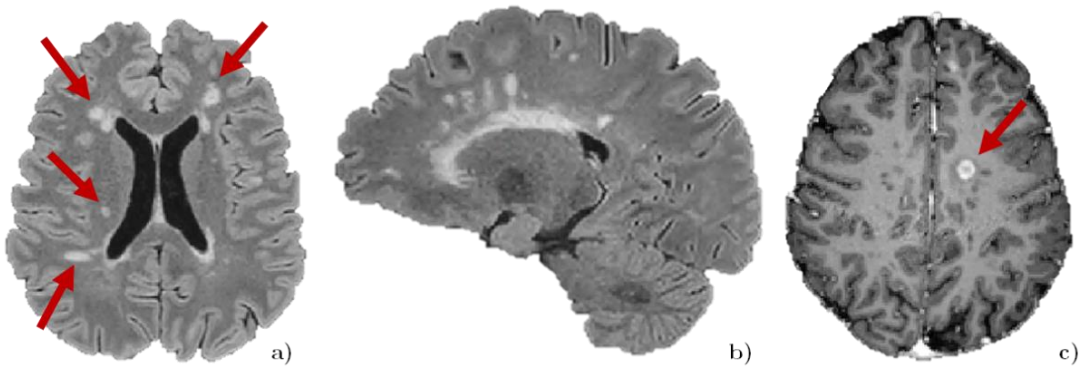

Figure 1: WM lesions in different MR images.

a) FLAIR image with MS typical WM lesion pattern in axial view; b) FLAIR image in sagittal view with MS typical lesion patter (Dawson´s fingers); c) contrast enhanced T1w image with Gadolinium enhancing lesion (red arrow); courtesy of the Dept. of Neuroradiology, TU Munich.

Gadolinium-enhancement of white matter lesions

The blood-brain barrier (BBB) prevents the intrusion of peripheral blood cells or potentially harmful molecules into the sensitive brain tissue. Inflammation can cause increased permeability of the BBB and thus enable the entry of peripheral cells, e.g. to remove cell debris and repair damaged tissue (Albrecht et al., 2016). By default,

disruption of the BBB is depicted by gadolinium-based contrast agent (GBCA) enhanced MRI (Figure 1c). Normally, GBCA molecules are unable to pass the BBB. If pre and post contrast enhanced MRI show changes, this hints to BBB disturbance and therefore neuroinflammation (Albrecht et al., 2016; Gaitan et al., 2011). This is especially true for new or enlarging lesions, since contrast enhancement persists typically for 2-6 weeks (Cotton et al., 2003).

Enhancement patterns vary, probably according to the type of initial BBB injury or time between GBCA injection and MRI scan, but no clear histological differences have been found between ring-like, open-ring or nodular appearances of enhanced lesions (Bruck et al., 1997; Gaitan et al., 2011; Lassmann, 2011).

The previous concept of GBCA entering the brain via the disrupted BBB, followed by a complete washout of GBCA after some time was challenged by recent histological studies demonstrating long term accumulation of Gadolinium (Gd) after repetitive GBCA application. This might point towards a potential risk of unfavorable long term effects (Kanda et al., 2017).

Grey matter and spinal cord lesions

In recent years, MS research has focused additionally to WM lesions in the brain on lesions in the spinal cord and on demyelination of the grey matter (GM), which plays an important role, especially in chronic phases of the disease (Bo et al., 2003; Kutzelnigg et al., 2005).

Inflammation might be the key driver of grey matter demyelination (Filippi et al., 2019). Histopathological studies showed monocytes, B- and T-cells within cortical GM and overlying meninges (Lagumersindez-Denis et al., 2017; Magliozzi et al., 2010), as well as microglial activation throughout the entire cortex (Herranz et al., 2016). GM demyelination varies in extent and location: neocortical areas are particularly affected (up to 40% demyelinated tissue) as reported in histopathological studies (Carassiti et al., 2018). Other GM regions (e.g. deep GM, cerebellar cortex)

are demyelinated less, 30% of affected tissue on average (Gilmore et al., 2009; Vercellino et al., 2009).

MS does not only affect the brain, but also the spinal cord. Thus, besides technical difficulties, spinal cord MRI as standard assessment of MS diagnosis can be valuable, if there are only few brain lesions (Thompson et al., 2018b). Moreover, spinal lesions are very typical for MS and can help to exclude alternative diagnoses such as vasculitis (Filippi et al., 2016). In several studies, spinal lesion load was correlated to disability in MS patients (Kearney et al., 2015; Valsasina et al., 2018).

Brain atrophy

Besides the mentioned inflammatory components of MS, degenerative factors can also be displayed with MRI (Figure 2). Cerebral and spinal volume change can occur within a relatively short period of time already in early disease stages. This change results from brain and spinal atrophy and leads to widening of the inner and outer CSF compartments (Filippi et al., 2012; Rocca et al., 2017).Virtually all mechanisms of MS-related tissue damage are assumed to contribute to neurodegeneration and, hence, to brain atrophy, which is most pronounced in brain GM. Yet, reliable determination of brain atrophy at the single subject level is currently not possible. Nevertheless, the MAGNIMS consortium recently published guideline recommendations for the standardization of the use of atrophy measures in clinical routine (Sastre-Garriga et al., 2020). The recommendations mainly focus on the predictive value of atrophy measures on diseases severity, as well as on monitoring therapeutic effects via disease modifying drugs. The consortium highlights the evidence for the correlation between global brain and cervical volume (change) and disability for all MS phenotypes and the resulting importance of atrophy measures in clinical practice (Sastre-Garriga et al., 2020). Additionally, measuring whole brain atrophy rate after 12 months under disease modifying therapy is recommended as secondary outcome parameter in clinical trials.

To sum up, atrophy measures are a good predictor for disease progression, but for inclusion into the clinical practice, more research is needed in this relatively young field of MS research. Unlike atrophy measures, lesions in brain and spinal cord have been established as diagnostic tools for many years. The following section describes this diagnostic workup in more detail.

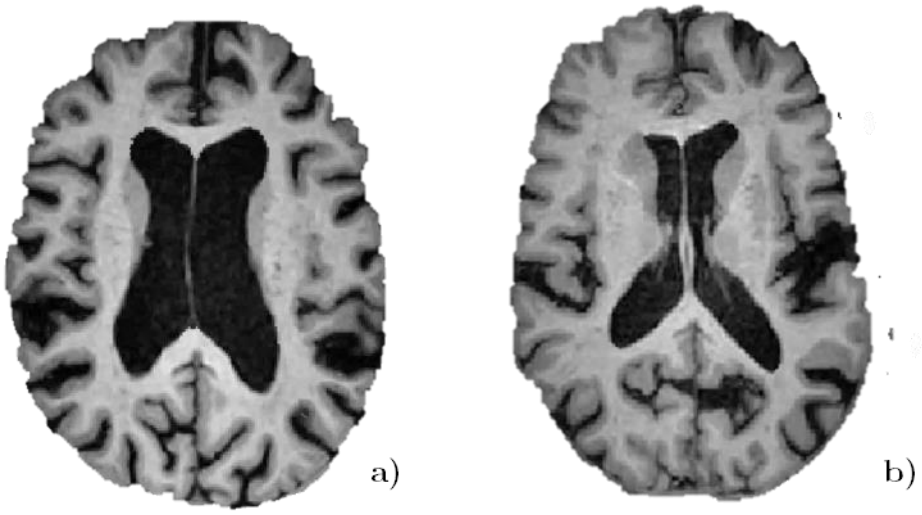

Figure 2: Atrophy in MS patients.

Two axial slices of T1w MRI from MS patients with high atrophy are shown. Note the typical widening of inner (a) and outer (b) CSF compartments. CSF, cerebro - spinal fluid; T1w, T1-weighted; courtesy of the Dept. of Neuroradiology, TU Munich.

1.2.2 Diagnostic criteria

Decades ago, Charles Poser stated that the diagnostic criteria for MS have, since the definition of the disease by Charcot, reflected the advances in understanding this disease, hand in hand with the technological progress (Poser & Brinar, 2004). From pure clinical assessment of symptoms in times of Charcot, the first ideas for standardized diagnostic criteria were proposed in 1982 and added the paraclinical tools of electrophysiological tests, CSF analysis and MRI to the diagnostic workup (Poser et al., 1983). The Poser criteria were, for the first time, able to unify terminology into clinical or laboratory definite MS and probable MS. They were

accepted worldwide, not only for the diagnosis in clinical routine, but also for clinical trials and epidemiological studies.

The 2001 proposed diagnostic criteria by McDonald and colleagues prioritized brain MRI as paraclinical tool to diagnose MS for the first time (McDonald et al., 2001). Since then, the International Panel on Diagnosis of Multiple Sclerosis has regularly published revisions of the McDonald criteria (Polman et al., 2011; Polman et al., 2005; Thompson et al., 2018b), allowing earlier, more sensitive and equally specific diagnosis (Brownlee et al., 2017).

Besides objective clinical evidence, which is a demyelinating attack in most instances, there are two main requirements for the diagnosis of MS: dissemination in space (DIS) and dissemination in time (DIT). DIS is defined as occurrence of lesions in distinct anatomical regions of the CNS, indicating a multifocal inflammatory CNS process. According to the latest revisions (Thompson et al., 2018b), DIS can be demonstrated by one or more characteristic T2w hyperintense lesions in two or more of the typical regions (periventricular, juxtacortical/cortical, infratentorial, spinal cord). DIT describes the development of new lesions over time, demonstrated by the concurrent existence of enhancing and non-enhancing lesions at the same time or by any new T2 hyperintense lesion on follow-up MRI, irrespective of the timespan between scans (Thompson et al., 2018b).

Given the leading role of MRI for the diagnosis of MS in the last decades and despite, or maybe because of, the fast progress of this technology, relevant questions to current clinical practice have remained unanswered. Two of these were addressed in this thesis.

1.2.3 Is there a size threshold for white matter lesion detection in MS?

Certainly, the WM lesion count, derived from brain MRI, has become the most important paraclinical feature to support the diagnosis of MS and to monitor its course (Sormani & Bruzzi, 2013; Thompson et al., 2015). But how is a WM lesion defined exactly? Can even the tiniest T2w hyperintense spot in the MR image be regarded as a WM lesion? The latest revision of the McDonald criteria for the diagnosis of MS defines a WM lesion as "An area of hyperintensity on a T2-weighted or proton-density weighted MRI scan that is at least 3 mm in long axis" (Thompson et al., 2018b). A minimum WM lesion size threshold of 3 mm in diameter (D) was stipulated in the past – assumingly because of technical constraints such as a slice thickness of 3 mm or more, a lower field strength and the application of sequences, which were not always optimized for WM lesion detection. Remarkably, a study cited in the 2001 consensus paper from the International Panel (McDonald et al., 2001) used an even larger threshold of 6 mm in D per WM lesion (Barkhof et al., 1997). In 2006, Swanton and colleagues, whose results contributed essentially to the later diagnostic guidelines (Polman et al., 2011), explicitly stated that the issue of a WM lesion size threshold is not resolved (Swanton et al., 2007). Although Swanton and colleagues asserted that 'a minimum lesion size may increase the specificity', they doubted that a minimum WM lesion threshold is necessary at slice thicknesses of 3 to 5 mm (Swanton et al., 2007). Later versions of the diagnostic criteria for MS (Polman et al., 2011; Polman et al., 2005; Thompson et al., 2018b) designated a minimum WM lesion size threshold of 3 mm in D, which – to the best of the author's knowledge – is not evidence-based and has never been subject of scientific investigation. Moreover, this specification loses its rationale for images of higher resolution and might have fallen behind the growth of technological possibilities of structural MRI. When applying a minimum WM lesion size threshold of 3 mm, 3

Tesla (T) scanners do not seem to be superior to scanners of lower field strengths regarding the diagnosis of MS (Hagens et al., 2018).

Of note, the choice of a minimum WM lesion size threshold may be critical. On one hand, when choosing an unnecessarily high WM lesion size threshold, meaningful disease-related information may be missed out. Given the availability of three-dimensional (3D) high resolution sequences at 3 T scanners nowadays, this possibility seems even more conceivable (Loria, 2016). On the other hand, small hyperintensities within cerebral WM on T2w sequences, i.e. WM lesions or WM changes, indistinguishable from those, are a common finding, not only in MS patients, but also in other populations such as in aged people or in subjects with high blood pressure (de Leeuw et al., 2002) or dementia (Brickman et al., 2015; Prins & Scheltens, 2015). A study, including more than 1000 healthy people older than 60 years, found that lesions as small as 1 - 3 mm in D constituted the majority of all WM lesions (de Groot et al., 2000). Another study showed that even middle-aged healthy participants without cognitive deficits or neurological history had WM lesions (Peng et al., 2016). Thus, although technically feasible, the inclusion of WM lesion smaller than 3 mm in D into the diagnostic criteria of MS could also lead to a precarious loss of specificity.

1.2.4 How safe is application of gadolinium-based contrast agents in MS?

MRI contrast agents are pharmaceutics used to improve visibility of certain body structures or pathological changes in MRI by enhancing tissue contrast (Weishaupt et al., 2006b). GBCA contain the heavy metal Gd, a paramagnetic substance which is toxic in its free state (Schild, 2012). For this reason, contrast agents use a ligand (chelate) to capsulize the Gd ion. Regarding the chelate moiety, two classes can be distinguished. Linear open-chain and cyclic chelates, which “cage” the Gd ion in a

pre-organized cavity (Port et al., 2008). Although the stability of GBCA depend on their kinetic, thermodynamic and conditional stability, the structural difference also has impact on the stability of the Gd chelate. Linear GBCA show lower binding affinity than cyclic ones and are therefore more likely to decompose (Bellin & Van Der Molen, 2008). As described previously (see section 1.2.1), in healthy humans, contrast media are not able to cross the BBB, thus contrast enhancement indicates indirectly pathological disruption of the BBB (e.g. through inflammation). This mechanism is used as a diagnostic tool mainly to detect neoplasms and inflammations (Weishaupt et al., 2006b). In MS patients GBCA are used in the diagnostic process for example to prove DIT with only a single MRI scan, since simultaneous presence of Gd-enhancing (freshly inflamed) and non-enhancing lesions point towards different dates of origin (Thompson et al., 2018b). GBCA can help to increase the sensitivity of lesion detection in both diagnosis and follow-up (Filippi et al., 1999; Miller et al., 1993). In addition, GBCA administration can be used to assess the acuteness of lesions (newly emerging inflammation) under immunomodulatory therapy, since Gd enhancement corresponds to a young lesion age (Cotton et al., 2003).

Traditionally, GBCA were considered to be the safest contrast agents with a very low rate of adverse events and the Radiological Society of North America estimates that worldwide more than 100 million patients received GBCA over the past 25 years (Radiological Society of North America, 2018). This image was challenged, as the first reports in 2006 linked GBCA administrations to nephrogenic systemic fibrosis, a rare disease that affects patients with renal failure (Grobner, 2006; Marckmann et al., 2006). Roccatagliata and colleagues first described T1 hyperintensity in MS patients (Roccatagliata et al., 2009). This study focused on signal abnormalities in the basal ganglia and dentate nucleus (DN), areas suspected to be involved in GM changes in MS. The authors detected T1 hyperintensity in the DN which was linked to the disease course (secondary progressive) of MS, as well as to increased clinical

disability, lesion load and brain atrophy (Roccatagliata et al., 2009). A later case study indicated, however, that hyperintensity on unenhanced T1-weighted (T1w) images can also be detected in patients with mild disability and low lesion load (Absinta et al., 2011). Other studies confirmed that hyperintensity in the DN and globus pallidus (GP) rather correlates to a history of brain irradiation, than to clinical factors (Adin et al., 2015; Errante et al., 2014; Kanda et al., 2014; Kasahara et al., 2011). From today`s perspective, this measurable signal intensity increase in unenhanced T1w sequences most likely reflects Gd deposition as demonstrated by post-mortem histopathological studies (Kanda et al., 2015a; McDonald et al., 2015). Free Gd was accumulated after intravenous infusion of GBCA in brain specimen of DN, GP, cerebellar WM, frontal lobe cortex and frontal lobe WM, even in subjects without renal dysfunction. The Gd concentration in the DN and GP specimen was significantly higher, than in other brain regions (Kanda et al., 2015a).

Gd deposition is, to some degree, accessible to investigation in vivo, even longitudinally and even by analysis of T1w images derived in clinical routine (Figure 4 a and b). Of note, patients with MS may be especially vulnerable to potential long-term effects of Gd deposition in the brain as repeated MRI scans over many years are frequently indicated to monitor disease modifying therapies. Further, intervals between scans are mostly longer than in other populations that have been studied with regard to Gd deposition in the brain such as patients with tumors (Behzadi et al., 2018; Kanda et al., 2014; Kanda et al., 2015b; Radbruch et al., 2017; Radbruch et al., 2015; Weberling et al., 2015). MS patients may therefore show different kinetics and distribution of GBCA accumulation.

Results from a follow-up study with MS patients indicate that T1 hyperintensities in the DN are only associated with linear GBCA administration, but not to macrocyclic ones (Schlemm et al., 2017). A systematic comparison of the contrast agents was done in an animal study, replicating that repeated linear, but

not macrocyclic GBCA application enhanced contrast in the DN (Jost et al., 2016). Contrary, further research in human patients revealed an increased signal intensity within DN and GP also after repeated application of macrocyclic GBCA and a correlation between the signal and the cumulative dose of the GBCA (Stojanov et al., 2016).

This inconsistent association between chelate type and Gd deposition, the focusing on certain brain areas in previous studies and the unknown kinetic aspects for long time periods show that more systematic research is needed for a better understanding of GBCA accumulation in MS patients.

1.3 Aims and outline

1.3.1 Project 1: Minimal white matter lesion size threshold in MS

The first project aimed to find an evidence-based WM lesion size threshold at magnetic field strength of 3 T for the diagnostic criteria and evaluation of MS. We therefore first compared patients with RRMS to control subjects (CS) with regard to WM lesion count and distribution of WM lesion sizes. We decided to only include patients suffering from RRMS, since the relapsing-remitting course is the most common disease course in MS (Pugliatti et al., 2006). We expected the variability of lesion sizes within and across RRMS patients to be sufficiently high and thus representative to determine a WM lesion size threshold. Second, we correlated the total WM lesion volume with the EDSS score, representing severity of clinical symptoms and impairment in MS patients. We further correlated WM lesion volume with thalamic volume, which is known to be a good predictor of MS related atrophy (Cifelli et al., 2002; Thompson et al., 2015). The same correlations were performed with the volume of small WM lesions, defined as those WM lesions smaller than 3 mm in D, in order to search for an MS-related signal of small WM lesions. Third, we calculated odds ratios (OR) across WM lesion sizes and determined a WM lesion

size threshold via receiver operating characteristic curve (ROC) analysis. Finally, all analyses were done twice, i.e. in a discovery and replication cohort, with MR images acquired at 3 T scanners from two different vendors.

1.3.2 Project 2: T1 intensity change after administration of gadolinium-based contrast agents

The second project investigated Gd deposition in the brain after administration of linear and cyclic GBCA in patients with MS. According to recent evidence, Gd deposition is, to some degree, accessible to investigation in vivo, even longitudinally and even by analysis of T1w images derived in clinical routine. This study followed and adapted this approach with data from a large cohort of patients with MS. Our main hypothesis was that linear GBCA would more likely cause deposition in the brain than the cyclic GBCA. Changes in T1w signal intensity in unenhanced T1w MPRAGE images were studied not only by region of interest analysis of the DN but also by whole brain analyses. We also studied kinetic aspects of Gd deposition.

1.3.3 Publication of project results

The results of both projects have been published in peer reviewed scientific journals as original articles separately for project 1 (Grahl et al., 2019) and project 2 (Grahl et al., 2020). These articles are connected in this secondary publication to unify the findings of MRI in the diagnostic process of MS from two different angles and to set them into a broader perspective.

2 Methods

2.1 Overview of the methods

This section provides an overview of the methods and techniques used in this thesis. First, the principles of structural MRI are explained briefly; second, the challenges in processing MR images from MS patients are described in more detail.

2.1.1 Principles of structural MRI

MRI is an indirect and non-invasive technique. It enables to image and analyze anatomical brain structures in vivo in humans. It is based on the magnetic resonance (MR) principle and on magnetization properties of water molecules. When a subject is placed in an MR scanner, a strong magnetic field (60,000 times stronger than earth`s magnetic field) is applied to align the water protons in the human body along this magnetic field (Weishaupt et al., 2006a). This orientation is afterwards perturbed by the application of a radiofrequency (RF) pulse in a certain frequency (repetition time; TR), causing the protons to align in the direction of the RF. The nuclei return (relax) to their previous alignment of the magnetic field and emit RF energy during this process, which is recorded by the MR scanner (echo time; TE). Since different tissue types have different chemical composition and water content, they differ in relaxation times and their signal varies (Weishaupt et al., 2006a).

The most common MR sequences are T1w and T2w sequences and they have also been used in this thesis. T1w images are produced by short TE and TR, whereas T2w images are produced by longer TE and TR. As, e.g. an MS WM lesion is a region of increased water content, they have a strong signal on T2w MRI (hyperintense) and low signal on T1w MRI (hypointense). FLAIR is similar to a T2w sequence except that an inversion pulse is applied before the excitation pulse which selectively suppresses the CSF signal (De Coene et al., 1992). This way, the contrast

between bright abnormalities (such as lesions) and CSF is intensified, and FLAIR has become the most important sequence for the detection of lesions in MS pathology (Filippi et al., 1996; Wattjes et al., 2006). The application of three-dimensional (3D), instead of two-dimensional (2D), sequences has not only further improved the detection of lesions in the brain, but the measurement of atrophy as well (Hu et al., 2019). 3D scans have several advantages over their 2D counterparts: they have isotropic voxel, better spatial resolution and they can be reformatted without comprising image quality. They also facilitate analyses of lesions and atrophy across multiple timepoints (Chagla et al., 2008; Vrenken et al., 2013). In contrast to 3D FLAIR images, 2D FLAIR images are often acquired with interslice gaps of up to 1.5 mm, increasing the probability of overlooking especially small lesions (Bink et al., 2006). Thus, 3D FLAIR images allow detection of much smaller lesions increasing the detection of WM hyperintensities up to 74%, compared to 2D images (Bravo et al., 2014; Patzig et al., 2014). The major disadvantage of 3D imaging, the prolonged scanning time, is alleviated by recent techniques accelerating image acquisition time.

2.1.2 Preprocessing structural MR images

After acquisition of images at the scanner and before analyzing them, images need to be preprocessed. The aim of various preprocessing steps is to improve image quality, to normalize them in order to set them in a standardized geometric space and to account for individual differences in head size (Manjón, 2017). Typical preprocessing steps for structural images are: denoising, registration and resampling, inhomogeneity and bias correction as well as normalization and segmentation.

MR images are inherently disturbed by random noise from the MRI scanner (Manjón, 2017). The main sources of noise during MR image acquisition are thermal noise from the scanned object, stochastic variation, eddy currents, or motion. The

denoising step aims at reducing noise while maintaining the original resolution with various methods (Mohan et al., 2014).

Registration is a method to map different images from the same subject into the same stereotactic space and to correct for motion artifacts during the acquisition process (Zijdenbos et al., 2002).

Intensity inhomogeneity, or bias field, is a typical MRI artifact, resulting from equipment limitation and patient-induced electrodynamic interactions. This bias, although mostly not a problem for visual inspection of the images, can cause misclassification in the segmentation step (which is based on intensity variation of different tissue types) and thus needs to be corrected. For bias field correction methods, a priori knowledge of the bias field distribution and model-based methods are used (Ashburner & Friston, 2007; Van Leemput et al., 1999).

Normalization is another spatial transformation step, since intersubject analyses of brain changes require images to be in the same normalized stereotactic space (Friston et al., 1995).

Segmentation is usually a later step in MR image preprocessing and is defined as the assignment of each voxel to a certain tissue class (Ashburner & Friston, 2007). Most commonly, segmentation is based on Gaussian models incorporating a priori knowledge on the probability for a certain tissue type in each voxel (Ashburner & Friston, 2007).

2.1.3 Challenges for preprocessing structural MR images in MS

Standard automated segmentation can be problematic in MS, because of multifocal WM hyperintensities, the hallmark of MS. In T1w images, usually used for segmentation, the intensity of WM lesions is darker than surrounding WM intensity and frequently closer to GM intensity resulting in misclassification of WM lesions as GM. This may not only lead to an overestimation of GM but also severely disturb

other processing steps (Chard et al., 2010). WM lesions might slightly modify the tissue intensity histogram, which is used to set cut-off values for separation of tissue types (Chard et al., 2010). In other words: if the segmentation algorithm correctly classifies WM lesions as WM, average intensity of WM drops and shifts WM cut-off values into darker GM regions, leading to overestimation of WM volume and underestimation of GM volume (Chard et al., 2010). Studies report that the presence of WM lesions may bias image registration and normalization as well (Brett et al., 2001; Sdika & Pelletier, 2009). Especially rigid methods of registration, which are fast and relatively robust, are unable to take into account small variations and thus registration may fail (Diez et al., 2014). To overcome these issues, several studies proposed to fill WM lesions with intensity values, similar to normal WM intensity values before registration and tissue segmentation (Battaglini et al., 2012; Chard et al., 2010; Valverde et al., 2014). For this procedure, WM lesion identification and segmentation is necessary first.

Currently manual labelling and semi-quantitative measures remain state of the art for WM lesion assessment. As lesions can be numerous and have fuzzy boundaries, creating ambiguity in their labelling process, this approach is very cumbersome, time-consuming and prone to high variability between the raters. Therefore, automated WM lesion segmentation has become a commonly accepted alternative for processing large datasets in the context of research projects. Automated lesion segmentation allows to produce completely reproducible, efficient and rater bias free lesion maps. The lesion segmentation toolbox (LST) (Schmidt et al., 2012) is one automatic method of lesion segmentation. In this thesis, LST was the software of choice for both projects. LST segments the lesions and generates a lesion-probability map, which is the basis for lesion filling according to the work of Chard and colleagues (Chard et al., 2010).

LST requires a FLAIR and T1w image of each subject as input. In the first step, preprocessing with existing software (SPM12 and CAT12) is done. T1w and FLAIR images are bias corrected and registered with linear and nonlinear transformation. Further, the T1w image is segmented into three tissue classes (WM, GM and CSF) in native space, using partial volume estimate label. Second, intensity distribution in the FLAIR image is calculated for all three tissue classes. Hyperintense outliers are binarized, stored in lesion belief maps and serve as seed point for the lesion growing algorithm. Third the lesion growth model expands the lesion belief maps to lesion probability maps. Iteratively, the algorithm checks for intensity changes in neighboring voxels and assigns a likelihood of belonging to the lesion or not to each voxel. Validation via semi-automated manual tracing of the lesion showed good agreement (Schmidt et al., 2012). High correlation between manual annotation and automated LST segmentation was confirmed by other research groups using a different scanner (Egger et al., 2017).

2.1.4 Image acquisition and processing workflow

The general workflow for processing MR images in both projects is depicted in Figure 3. Project specific aspects are described in sections 2.2.2 and 2.3.2.

Two high resolution MRI sequences (3 T, Scanner: Achieva, Philips, Netherlands) were used: 1) 3D gradient echo T1w sequence (voxel size = 1mm isotropic, TR = 9 ms, TE = 4 ms. 2) 3D turbo-spin echo T2w FLAIR sequence (voxel size = 1.0× 1.0× 1.5 mm; TR = 10,000 ms; TE = 140 ms; TI = 2750 ms). All images were preprocessed and normalized with SPM12 and its toolboxes CAT12 (http://www.neuro.uni-jena.de/cat/index.html) and LST 2.0.15 (http://www.statisticalmodelling.de/lst.html). Default options were applied, if not stated otherwise. After co-registration to the T1w image in native space, the FLAIR image was used to segment T2-hyperintense WM lesions by the lesion growth

algorithm of LST as described above (Schmidt et al., 2012). Next, the resulting binary WM lesion maps in native space were projected onto the T1w image in which lesion voxels were removed and filled with normal WM intensity values (lesion filling algorithm in LST). These filled T1w images were normalized into the standard space of Montreal Neurological Institute (MNI) and segmented into GM WM and CSF using voxel-based morphometry of the CAT12 toolbox. Volumes of GM, WM, CSF were calculated with CAT12 from the respective normalized filled T1w images based on the atlases implemented in CAT12. WM lesion volume was extracted from binarized WM lesion maps in native space with LST. At all stages of processing, images were visually checked to ensure quality.

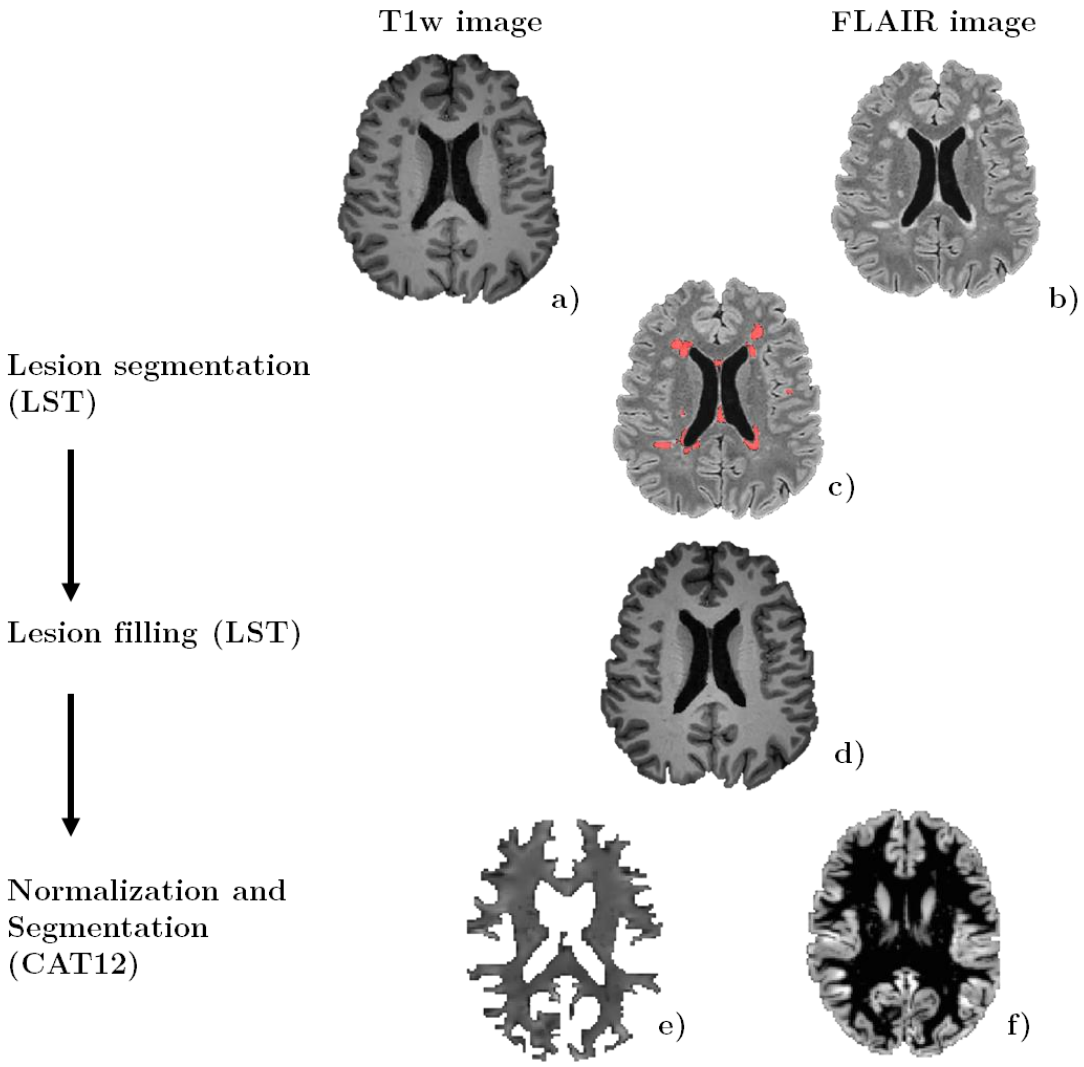

Figure 3: General workflow of processing MR images for MS patients in both thesis projects at one exemplary patient.

a) T1w MPRAGE image in native space; b) FLAIR image in native space; c) FLAIR image with overlaid LST-segmented lesion mask, lesions in red; d) filled T1w image; e) normalized WM image; f) normalized grey matter image.

2.2 Project 1: Minimal white matter lesion size threshold in MS

2.2.1 Participants

This retrospective study was approved by the ethics committees of center 1 (School of Medicine, TU Munich) and center 2 (School of Medicine, Johann-Gutenberg-University Mainz), respectively. The study was performed according to the declaration of Helsinki.

From each of the two different MS centers, we included data from patients with RRMS (MS group) as well as CS. We selected 87 CS (64.2% females; age = 36.4 +/- 9.8) from center 1 and 49 CS (55.1% females; age = 33.8 +/- 9.6) from center 2. Not all of them showed WM hyperintensities (86/87 in center 1 and 29/49 in center 2). Given that a considerable proportion of CS showed WM hyperintensities, which for simplicity will also be called WM lesions, and that the absence of WM lesions does not constitute a challenge in clinical practice, we included only CS with WM lesions and will only report data on the selected CS.

Demographic and clinical characteristics of both cohorts are given in Table 1. Patients from center 1 were recruited from an in-house observation study. In center 1 78 percent of the MS patients (MS1) were treated with disease-modifying drugs. MRI data of the CS group in center 1 (CS1) was taken from an in-house database of CS. Subjects included in this database were either scanned in the context of other imaging studies at center 1`s neuroimaging center as CS or in the context of medical examinations, performed because of transient headache or symptoms that retrospectively could not be related to a severe or chronic neurological disorder (e.g., transient sensory symptoms due to mechanical irritation of a peripheral nerve). MS2 patients were recruited from the clinical database of the Department of Neurology of center 2. MRI data of the CS group in center 2 (CS2) was taken from

the database of its neuroimaging center, which exclusively contained healthy subjects recruited as controls for imaging studies.

Subjects with neurological or psychiatric comorbidities were excluded, two MS2 patients had to be excluded due to motion artifacts in the structural MRI scans and one CS2 was excluded due to extensive WM abnormalities of unknown cause.

Two sample t-tests did not show significant differences in age between MS1 and CS1 and between MS2 and CS2; likewise, chi-square tests did not show significant differences in sex between MS1 and CS1 and between MS2 and CS2. The patient groups from both centers resembled each other (Table 1). By two-sample t-tests, no significant differences were found for age and disease duration. Yet, EDSS differed significantly between groups with higher scores in MS2 compared to MS1 ($p = 0.003$). Chi-square tests did not reveal a significant difference in sex between MS1 and MS2.

Table 1: Demographic and clinical parameters of cohort 1 and cohort 2

	Cohort 1		Cohort 2	
	RRMS	CS	RRMS	CS
n	116	86	115	29
Mean age in years (SD)	36.0 (9.8)	34.3 (7.0)	36.15 (11.7)	35.2 (9.5)
% female	64.7	75.6	67.0	55.7
Mean EDSS (SD)	1.3 (1.0)	n/a	1.8 (1.4)	n/a
Mean disease duration in years (SD)	3.17 (4.6)	n/a	4.68 (5.8)	n/a
% under disease modifying drugs	80		63.5	

CS, control subjects; EDSS, Expanded Disability Status Scale; n/a, not applicable; SD, standard deviation.

2.2.2 Image processing

MRI sequence parameters of center 1 were given in section 2.1.4. In center 2, two high resolution MRI sequences (3 T, Scanner: Trio, Siemens Healthcare, Erlangen, Germany) were used: 1) a 3D spoiled gradient echo T1w sequence (MPRAGE) (voxel size = 1 mm isotropic; TR = 1900 ms; TE = 2.5 ms, TI = 900 ms). 2) a turbo-spin echo T2w FLAIR sequence (voxel size 1.0 mm isotropic; TR = 5000 ms; TE = 388 ms, TI = 1800ms). Images from both centers were processed as described in section 2.1.4. At all stages of processing, images were visually checked to ensure quality. We used SPM12 and its toolboxes CAT12 (http://www.neuro.uni-jena.de/cat/index.html) and LST (lesion segmentation tool) 2.0.15 (http://www.statistical-modelling.de/lst.html) for lesion segmentation. Default options of SPM, CAT and LST were used, apart from lowering LST's minimum WM lesion size to two contiguous voxels. This corresponds to a volume of 2 mm^3 independent of the voxel sizes of the initial raw images. We chose this fully automated strategy for lesion segmentation since reliable manual segmentation of WM lesions down to a size of only two contiguous voxels is hardly feasible. After lesion segmentation in FLAIR images, T1w images were filled with normal WM intensity values, normalized and segmented. Volumes of GM, WM, CSF and thalamus were calculated with CAT12 from the respective normalized filled T1w images, based on the atlases implemented in CAT12. WM lesion volume was extracted from binarized WM lesion maps in native space with LST. Instead of the diameter as a 2D measure (most frequently used in the literature), we analyzed the 3D measure of volume to make full use of the information contained in our 3D sequences. For clarity, we also indicate the diameter as estimated for each lesion by $D = \sqrt[3]{(Volume * 6)/\pi}$.

To compare the image quality of both FLAIR sequences, we calculated the contrast-to-noise ratio (CNR = $\frac{\bar{x}_{WM\,lesion} - \bar{x}_{WM}}{\sigma_{WM}}$) and signal-to-noise ratio

(SNR = $\frac{\bar{x}_{putamen}}{\sigma_{putamen}}$) from 10 randomly chosen subjects from each center. Putamen was chosen as region of interest (region of comparison) for the CNR since its signal is not affected by WM pathology in MS and it is easily detectable. Putamen was identified semi-automatically by using the MNI structural atlas included in the software package FSLview 5.0.1 (https://fsl.fmrib.ox.ac.uk/fsldownloads_registration).

For quality assurance, WM lesion segmentation was checked visually for both centers. Additionally, we chose 6 subjects (3 MS, 3 CS) per center with a WM lesion number near the mean of their respective group and calculated individual values of lesion-wise sensitivity (i.e. detection rate = true positive WM lesion / (true positive WM lesion + false negative WM lesion)) and lesion-wise false discovery rate (i.e. false positive rate = false positive WM lesion/ (false positive WM lesion + true positive WM lesion)).

2.2.3 Statistical analyses

For statistical analyses, we used SPSS (Version 24, IBM) and Rstudio, version 3.2.3. Both cohorts (cohort 1 and cohort 2) were analyzed independently, no pooled statistical tests were used. WM lesions of the MS and CS group were compared with regard to volume and number for all WM lesions and only small WM lesions (D < 3 mm) separately by unpaired t-tests. We examined small WM lesions separately to reveal MS-related signals below the current convention of a minimum WM lesion size of 3 mm in diameter. The relationship between WM lesion volume and thalamic volume as well as EDSS score was investigated with partial correlation analyses, corrected for age and total intracranial volume. Again, we performed correlation analysis separately for all WM lesions and for only small WM lesions to reveal MS-related signals of small WM lesions compared to all WM lesions. Further, we correlated the counts of all WM lesions and small WM lesions. OR was assessed

to quantify the probability of occurrence of a certain WM lesion size in MS compared to CS. ROC analysis was used to identify an optimal minimum WM lesion size threshold to distinguish MS subjects from CS. ROC graphically displays the trade-off between sensitivity and specificity across a range of possible cut-off values or thresholds that discriminates best between two groups (Florkowski, 2008) – in our case between MS vs. CS. The trade-off is commonly estimated by the sum of specificity and sensitivity. In our case, each WM lesion of a volume below the cut-off is labelled 'no MS,' i.e. a WM lesion more likely not derived from an MS patient, whilst each WM lesion of a volume above the cut-off is labelled 'MS,' i.e. a WM lesion more likely to derive from an MS patient. Sensitivity is the rate of WM lesions from MS patients correctly labelled (true positives); specificity is the rate of WM lesions from CS correctly labelled (true negatives). The ROC analysis determines the optimal cut-off value (WM lesion threshold) maximizing the trade-off between sensitivity and specificity.

2.3 Project 2: T1 intensity change after administration of gadolinium-based contrast agents

2.3.1 Participants

This retrospective single center study was approved by the internal review board (School of Medicine, TU Munich) and performed in accordance with the ethical standards laid down in the 1964 Declaration of Helsinki and its later amendments. Patients had given written informed consent for the use of their MRI data for research projects. We included patients with MS (Table 2) and at least two MRI scans according to a standardized in-house protocol between 2009 and 2017 (described in section 2.1.4). Exclusion criteria were comorbidities possibly interfering with image analysis, lesions within our control region for scaling (see below) and

further GBCA administrations between pairs of scans (according to our hospital information system). In 2015, our standard changed from the linear GBCA gadopentetic acid (Magnevist®) to the cyclic GBCA gadoterate meglumine (Dotarem®). Of the 881 patients included, 428 received both linear and cyclic, 395 exclusively linear, 53 exclusively cyclic and 5 no GBCA. Standard dosage was used (0.1 mmol/kg body weight, up to 10 mmol total).

Table 2: Summary of demographic and clinical data

		Linear GBCA	Cyclic GBCA	No GBCA (control)	All conditions 1st scan	All conditions last scan
n		2718	385	130	3233	3233
Mean age (SD)		37.5 (10.4)	39.1 (10.6)	37.7 (9.8)	36.2 (10.6)	39.8 (10.9)
Sex (%female)		66.7	68.1	63.8	68.0	68.0
Mean EDSS (SD)		1.7 (1.7)	1.5(1.5)	1.3 (1.2)	1.6 (1.7)	1.6 (1.7)
Mean dis. dur. in years (SD)		3.7(4.3)	5.3 (5.0)	5.1 (4.5)	2.1 (4.6)	5.8 (5.3)
Mean n GBCA administration (SD)		5.4 (4.0)	1.4 (0.7)			
Diagnosis in %	CIS				28.7	11.8
	RRMS				66.8	83.3
	SPMS				2.8	3.5
	PPMS				1.5	1.5

CIS, clinically isolated syndrome; dis. dur., disease duration; EDSS, expanded disability status scale; GBCA, Gadolinium-based contrast agent; n, number; PPMS, primary progressive MS; RRMS, relapsing-remitting MS; SD, standard deviation; SPMS, secondary progressive MS.

2.3.2 Image processing

MRI sequence parameters (T1w, FLAIR) are given in section 2.1.4. All images were preprocessed and normalized with SPM12 and its toolboxes CAT (http://www.neuro.uni-jena.de/cat/index.html) and LST 2.0.15 (http://www.statistical-modelling.de/lst.html) with their default options resulting in T1w images which are bias-corrected, normalized to MNI space and their WM lesions are filled with intensities of normal appearing WM as described in section 2.1.4. Next, we defined the region of interest (DN) and the control region (pons). The DN mask of FSL's SUIT toolbox (https://fsl.fmrib.ox.ac.uk/fsldownloads_registration) was projected onto individual FLAIR images (normalized to MNI space after coregistration to the T1w images), since the contrast of the DN is higher in FLAIR sequences (hyperintense) than in T1w images. Median FLAIR intensity of the dentate nucleus region was calculated and only voxels with lower intensity than the median intensity (within the SUIT DN mask) built the final individual DN mask (Figure 4 c and d) to ensure a conservative DN mask.

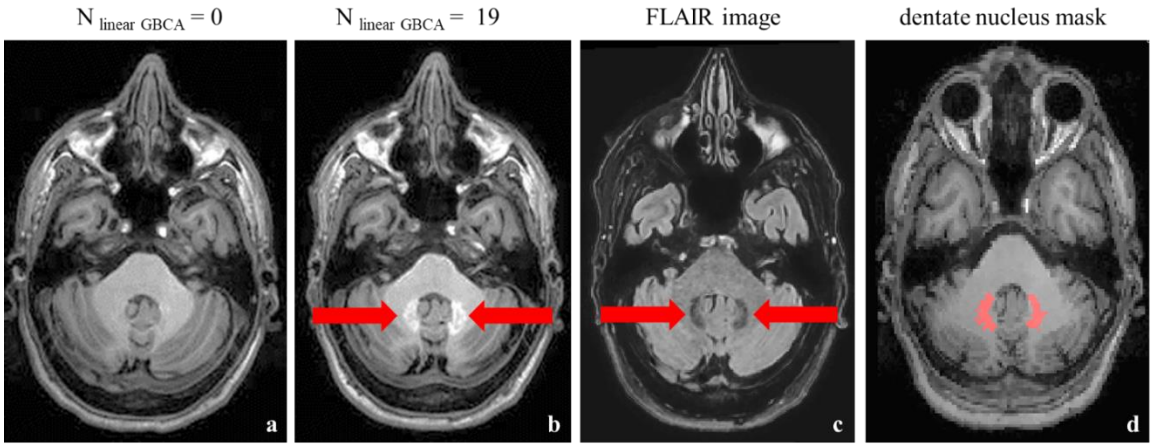

Figure 4: Example images of intensity change after GBCA application and DN mask.

A patient with visible T1w signal intensity increase within the DN is shown. Unenhanced T1w images were acquired in 2009 (a) and after 20 applications of linear gadolinium-based contrast agents (GBCA), in 2016 (b) where the DN appears brighter (arrows); from the FLAIR image (c) and the DN mask of FSL SUIT toolbox (not shown), the customized DN mask was generated and projected on the normalized T1w image (d, mask in red).

For scaling, median signal intensity within the control region pons was determined in a sphere of 5 mm in diameter around the MNI coordinate x = 0, y = - 26, z = - 36. FLAIR images were visually checked for WM lesions in the DN or P region. In case of WM lesions in these regions, images were excluded (n = 10) because WM lesions lead to signal changes, not intended to measure here. Individual DN and pons masks were projected on the unenhanced T1w image in MNI space, median voxel intensity was calculated for the respective regions and the DN-to-pons ratio (DN/P) was built. For regional analyses, DN/P values of two subsequent time points were subtracted (later minus earlier image). Resulting difference values were attributed to one of the three conditions (linear, cyclic or, as control, no GBCA). Figure 5 depicts an exemplary assignment of images of one patient to either of the three conditions. In total 2718 difference values were included in the linear condition, 385 in the cyclic condition and 130 in the control condition. For whole brain analyses, we calibrated the normalized and bias corrected T1w images by dividing voxel intensity values by their median pons intensity value. We then calculated difference images by subtracting the calibrated T1w images from two subsequent time points. Difference images were also attributed to one of the three conditions (linear, cyclic or control).

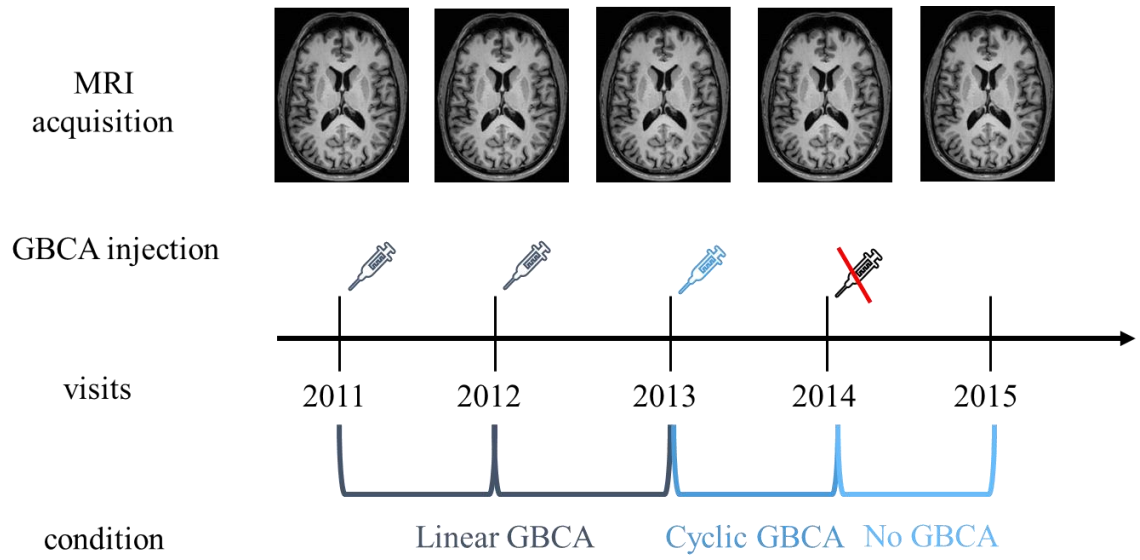

Figure 5: Study design of project 2.

The study design is illustrated by an exemplary patient. Gadolinium-based contrast agent (GBCA) was applied in 2011, 2012 (both linear GBCA), and 2013 (cyclic GBCA) but not in 2014. This patient contributes difference images between two subsequent timepoints to the linear GBCA condition (2011/2012; 2012/2013), the cyclic GBCA condition (2013/2014) and the control (i.e. no GBCA) condition (2014/2015)

2.3.3 Statistical analyses

We performed three types of analyses. Rstudio Version 1.0.143 (2017) was used and p-values < 0.05 were considered statistically significant. First, we explored the potential influence of several parameters on the T1w signal changes in the DN (of the difference images) such as number of previous GBCA administrations (i.e. testing for non-linear effects), age, and sex. Searching for GBCA-related changes of the MR signal in the control region pons that could disturb our analyses, we plotted the median pons intensity over the number of GBCA administrations separately for linear and cyclic GBCA. We further assessed the relationship between latest EDSS score and maximum number of GBCA administrations per person.

Second, we focused on the DN as increases in intensity after GBCA administration in this regions had been reported consistently (Adin et al., 2015;

Kanda et al., 2014; Radbruch et al., 2015; Stojanov et al., 2016). By one-sample t-tests within each condition, we tested whether mean signal intensity changes were significantly larger than zero. By two-sample t-tests, DN/P differences were compared between conditions. We also tested the hypotheses that GBCA deposition in the brain is reversible to some degree, which includes the observation of a washout of linear GBCA when followed by the administration of cyclic GBCA (Behzadi et al., 2018; Radbruch et al., 2016). Therefore, we additionally analyzed two subconditions of the conditions cyclic GBCA and no GBCA, including only difference images of subjects having received linear GBCA beforehand. This resulted in the subconditions 'cyclic GBCA after linear GBCA' and 'control after linear GBCA'. For example, the cyclic condition illustrated in Figure 5 contributed to the subsample 'cyclic GBCA after linear GBCA' as the second linear GBCA condition preceded the cyclic GBCA condition (2012/2013).

Third, we performed whole brain analyses to search for further areas with an increase of the T1w signal after GBCA administration. Whole brain voxel-based analysis was performed in SPM12 using the T1w difference images after smoothing with a Gaussian kernel of 4 mm full width at half maximum. Again, we performed one-sample t-tests against zero for each of the conditions and two-sample t-tests to compare conditions. Voxel-wise p-values < 0.05, after family wise error correction across the whole brain, were considered statistically significant.

3 Results

3.1 Project 1: Minimal white matter lesion size threshold in MS

As a first step, we visually compared MR images of the two scanner vendors. FLAIR sequences and, to a lesser extent, T1w images of the two vendors yielded different image impressions. Figure 6 illustrates the different appearance of images from the Philips Achieva scanner (cohort 1) compared to the Siemens Trio (cohort 2). The visual impression was underpinned by image quality measures. Images from the Philips Achieva scanner showed significantly ($p < 0.001$) lower contrast-to-noise and signal-to-noise ratios (mean CNR = 4.2 +/- 0.5; mean SNR = 5.6 +/- 1.2) than the Siemens Trio (mean CNR = 7.2 +/- 0.9; mean SNR = 9.2 +/- 3.0). Nevertheless, visual inspection of processed images showed that preprocessing and automated lesion segmentation performed consistently well. We tested WM lesion segmentation performance in six exemplary subjects per center. Lesion-wise sensitivity was 0.81 for center 1 and 0.79 for center 2; false discovery rate was 0.08 for center 1 and 0.11 for center 2.

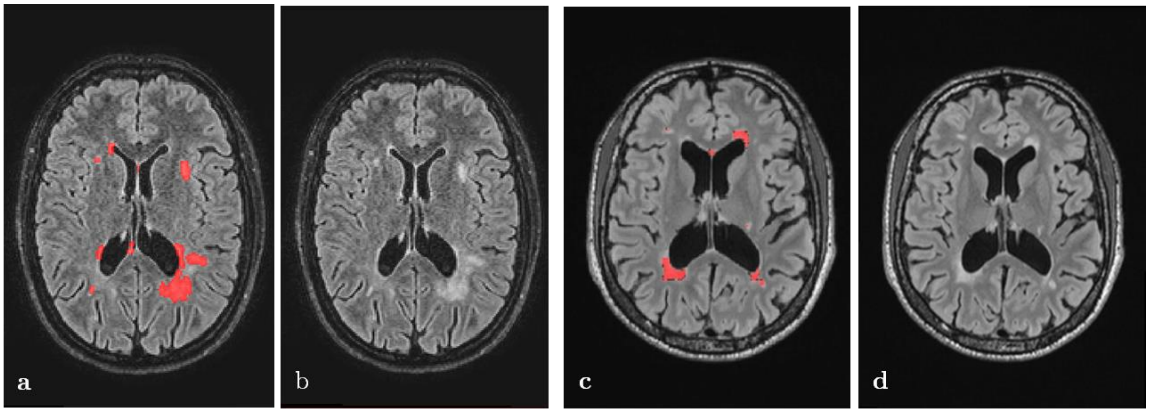

Figure 6: Examples of FLAIR images and lesion segmentation from two MS patients from two MS centers.

a-b) cohort 1. c-d) cohort 2. a/c) FLAIR image. b/d) FLAIR image with segmented white-matter lesions in red. Note the different appearance of images from the Philips Achieva scanner of cohort 1 (a/b) compared to the Siemens Trio of cohort 2 (c/d).

Next, we report results from the comparison of the two cohorts; only if significance of results differed between the cohorts, results are indicated separately. As expected (all p values < 0.001), both WM lesions in total and small WM lesions ($D < 3$ mm) occurred significantly less often and with lower mean volume in CS compared to MS (Table 3). On average, 8.6 WM lesions (48% small WM lesions) were counted in CS1 and 28 WM lesions (34% small WM lesions) were observed in MS1 patients (CS2: 1.4 WM lesions with 58% small WM lesions and MS2: 17.6 WM lesions with 19% small WM lesions). Compatible with the image impression, also average numbers of small WM lesions differed substantially between the scanner sites. In cohort 1, small WM lesions were more frequent, compared to cohort 2 (Table 3), suggesting higher sensitivity of the scanner from center 1. Yet, ratios of mean small WM lesion numbers between MS and CS was higher in cohort 2 (2.3 vs. 4.0), suggesting higher specificity of the scanner from center 2.

Table 3: White-matter lesion volume and number in MS patients and control subjects for cohort 1 and cohort 2

		Cohort 1		Cohort 2	
		RRMS	CS	RRMS	CS
N subjects		116	86	115	29
Total WM lesion volume (ml)	Mean (SD)	4.54 (5.57)	0.399 (0.439)	4.67 (8.28)	0.054 (0.084)
Total WM lesion number	Mean (SD)	28.17 (15.48)	8.710 (6.228)	17.63 (12.35)	2.28 (1.811)
Small WM lesion volume (ml)	Mean (SD)	0.87 (0.05)	0.0356 (0.029)	0.03 (0.03)	0.007 (0.009)
Small WM lesion number	Mean (SD)	9.46 (5.53)	4.150 (3.334)	3.29 (2.74)	0.79 (1.048)

CS, control subjects; N, number; RRMS, relapsing-remitting MS; SD, standard deviation; small WM lesion, WM lesion with D < 3 mm; WM lesion, white-matter lesion.

The average WM lesion count per subject increased with WM lesion volume, peaking at about 0.004 ml WM lesion volume for both CS and MS and then decreased continuously (Figure 7). Correlation of individual counts of small WM lesions and WM lesions > 3 mm across subjects was significant in the MS group (cohort 1/2: $r > 0.7$; p values < 0.001), i.e. the more small WM lesions an MS patient had, the more "large" WM lesions (> 3 mm) were present as well. However, in the CS group, the same correlation was found (cohort 1/2: $r = 0.6/0.7$; $p < 0.001$).

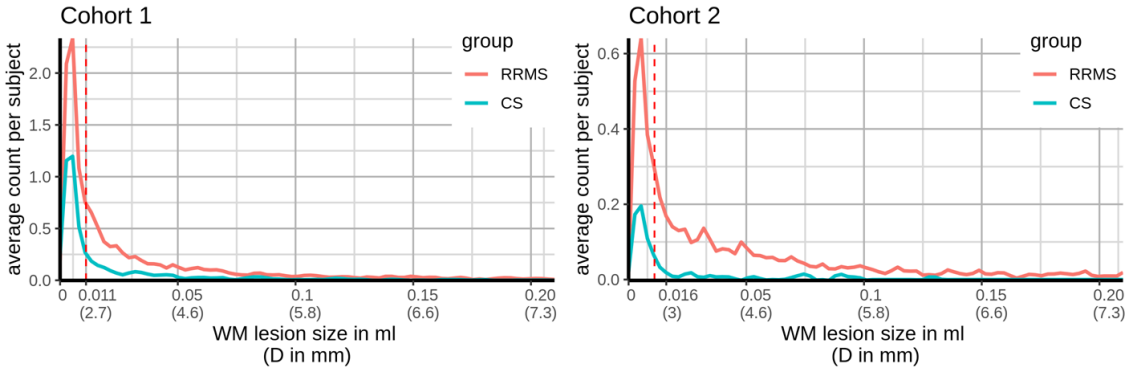

Figure 7: Frequencies of white-matter lesions by size.

By LOESS (LOcally wEighted Scatter-plot Smoother) plots, average white-matter (WM) lesion counts per subject (y-axis) are plotted across WM lesion sizes (x-axis) separately for control subjects (CS in blue) and patients with relapsing-remitting multiple sclerosis (RRMS in red). Counts of WM lesions peaked between 0.002 ml and 0.008 ml in MS and CS at both scanner sites and then approached zero. Dotted vertical lines display WM lesion size thresholds from receiver operator characteristics analyses. Cohort 1: threshold at V = 0.011 ml (D = 2.7 mm) and cohort 2: V = 0.016 ml (D = 3.1 mm).

Partial correlation analyses revealed that total WM lesion volume correlated positively with disability status (EDSS) and negatively with thalamic volume in both MS cohorts (Table 4). The latter correlation was significant in CS1 and showed a trend towards significance in CS2. In MS1, small WM lesions were significantly correlated to thalamic volume but not to EDSS (Table 4), whilst, in MS2, the volume of small WM lesions was significantly correlated to both thalamic volume and EDSS (Table 4). Volume of small WM lesions correlated only in CS1 with thalamic volume, but not in CS2. As expected, OR across WM lesion sizes increased in general (Figure 8) with an OR (cohort 1/2) of 2.1/5.25 at 0.015 ml (D = 3 mm) and an OR of 2.9/11.9 at 0.1 ml (D = 6 mm).

Table 4: Correlation analyses of white-matter lesion volume with disability and thalamic volume

	Cohort 1			Cohort 2		
Variable of interest	EDSS	Thalamic volume		EDSS	Thalamic volume	
Group	RRMS	RRMS	CS	RRMS	RRMS	CS
	r (p)	r (p)	r (p)	r (p)	r (p)	r (p)
Total WM lesion volume	0.214 (0.027)	-0.664 (<0.001)	-0.275 (0.012)	0.378 (< 0.001)	-0.627 (< 0.001)	-0.324 (0.08)
Small WM lesion volume	0.097 (0.320)	-0.487 (<0.001)	-0.274 (0.012)	0.228 (0.015)	-0.347 (< 0.001)	0.024 (0.91)

Correlations were corrected for age and total intracranial volume. D, diameter; p, p-value; r, partial correlation coefficient; small WM lesion, WM lesion with D < 3 mm; WM lesion, white-matter lesion.

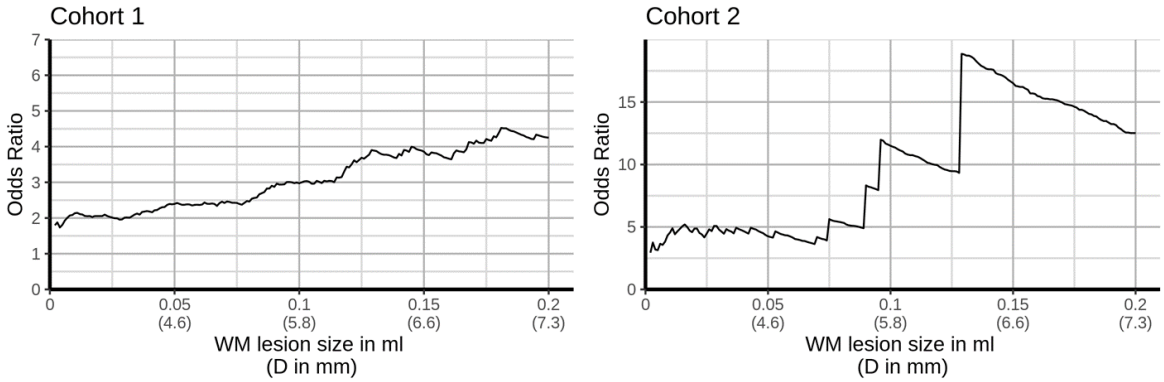

Figure 8: Odds ratios of white-matter lesion sizes.

Odds ratios derived from the relapsing-remitting MS groups and control groups (y-axis) are plotted across white-matter (WM) lesion sizes. Odds ratios increase with increasing WM lesion size. D, diameter.

ROC analysis revealed that the optimal discriminating WM lesion size threshold was 0.011/0.016 ml (D = 2.7/3.1 mm) for cohort 1/2. However, sensitivity (0.55/0.64) and specificity (0.62/0.70) were low, as well as the area under the curve (AUC = 0.62/0.73) for cohorts 1 and 2. Figure 9 depicts the trade-off between sensitivity and specificity across WM lesion sizes.

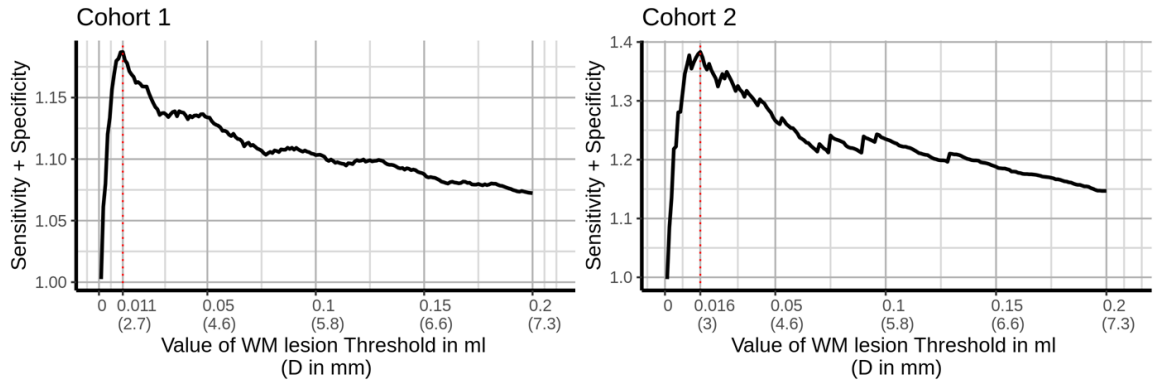

Figure 9: Receiver operating characteristic curve analyses for lesion sizes.

Modified receiver operating characteristic curve. The sum of specificity and sensitivity, reflecting the trade-off between the two parameters (y-axis), is plotted across thresholds of white-matter (WM) lesion sizes. A clear peak was detectable at 0.011 ml (D = 2.7, cohort 1) and 0.016 ml (D = 3.1, cohort 2), respectively. D, diameter.

3.2 Project 2: T1 intensity change after administration of gadolinium-based contrast agents

We did not find an indication that any of the potentially confounding parameters interfered with the signal intensity changes after administration of GBCA in a meaningful way (Figure 10). In particular, the signal change between subsequent scans was almost independent of the number of GBCA administrations beforehand. Correlation analyses (Figure 10, upper panel) showed a significant correlation (linear: $R2 = 0.004$; $p = 0.001$) of the signal changes after linear GBCA, but not after cyclic GBCA ($R2 = 0.0004$; $p = 0.7$) with the number of GBCA administrations. Yet, the significant effect was very small explaining only 0.4 % of the variance of signal increase which justified our approach to analyze pairs of subsequent images (i.e. difference images). Further, neither age nor sex showed a correlation with the signal intensity changes after administration of GBCA (Figure 10, middle panels). Moreover, the T1w signal of the control region pons varied but did not change systematically with respect to the number of previous GBCA administrations (Figure 10, lower panel, $R2 = 0.0001$, $p = 0.5$). As expected, EDSS score correlated with maximum number of GBCA administration per subject ($R2 = 0.01$, $p = 0.005$).

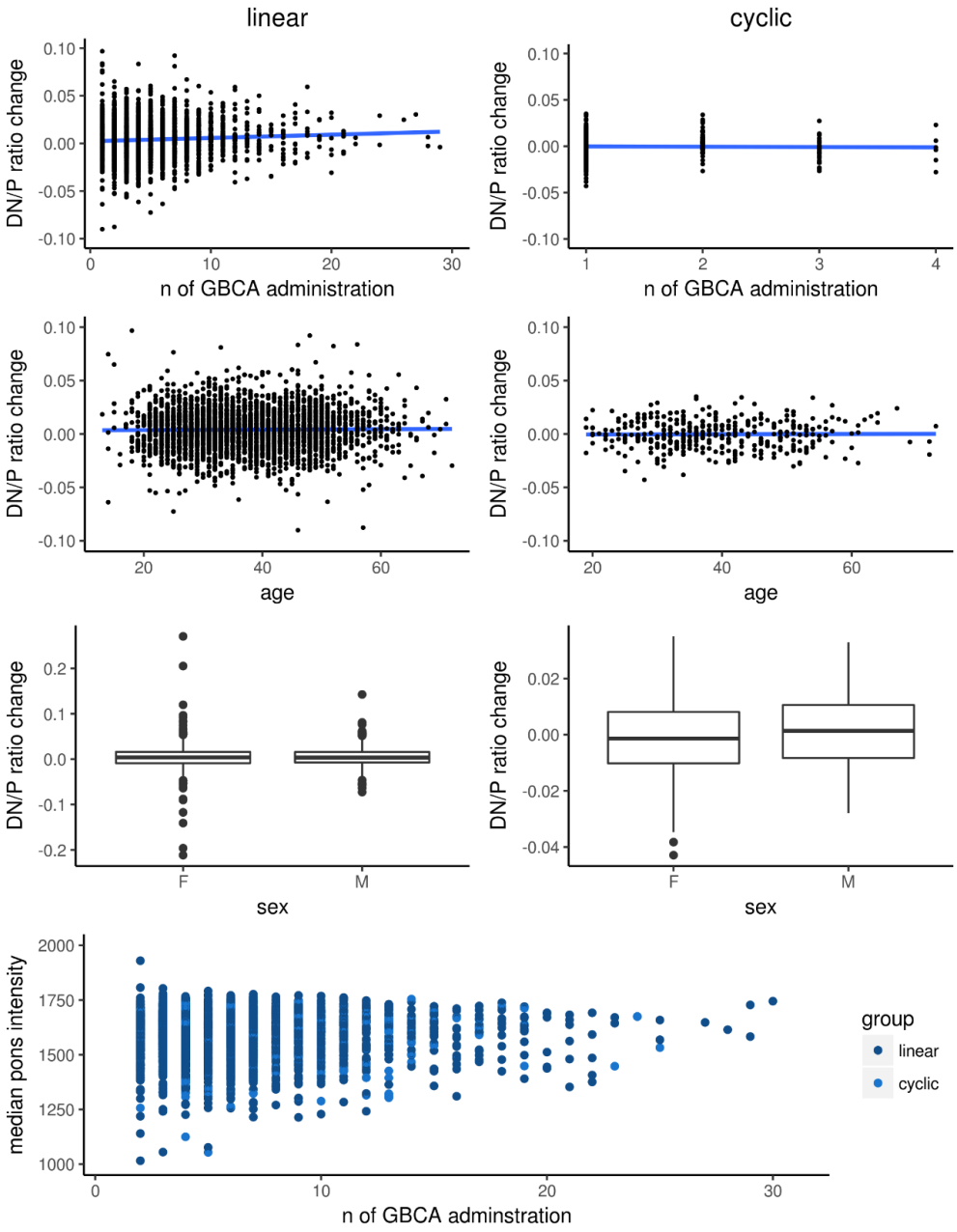

Figure 10: Potentially confounding variables for analyses of GBCA effects.

Parameters potentially interfering with signal intensity changes after application of gadolinium-based contrast agent (GBCA) were analyzed. In the upper three panels, changes (per pair of consecutive images) in the intensity ratio of the dentate nucleus (DN) and pons (P) after application of linear (left column) and cyclic (right column) GBCA are plotted against the number of applications, age, and sex; Pearson`s correlation of signal change and number of previous GBCA administrations in the linear condition was significant, but very small ($R2 = 0.004$), no systematic influence was observed for the cyclic condition as well as for age and sex in both conditions. In the lower panel, the intensity values of the control region (pons) is plotted against number of previous GBCA administration without an indication of a systematic shift (linear GBCA in dark blue, cyclic GBCA in light blue) of the T1w signal over time ($R2 = 0.0004$). DN/P, DN-to-pons ratio; F, female; M, male; n, number.

Our regional analyses of the DN with one-sample t-tests revealed a significant increase of the DN/P ratio only after administration of linear GBCA (Figure 11). In extreme cases, this could be detected visually (Figure 4 a and b). Of note, when focusing on the other end of the spectrum, we found a DN/P ratio by summing up only the difference images after first time administration of linear GBCA (Figure 11). Comparing the conditions of different GBCA directly by two-sample tests, we found significantly higher increases of the DN/P ratio after administration of linear GBCA compared to cyclic and no GBCA (Figure 11). DN signal change did not differ significantly between the cyclic GBCA and the no GBCA group. Subcondition analyses (cyclic GBCA condition following linear GBCA condition, control condition following linear GBCA condition) did not reveal significant deviation from 0 in the one-sample t-tests (Figure 11), thus did not suggest a decrease of DN/P after the end of linear GBCA administration.

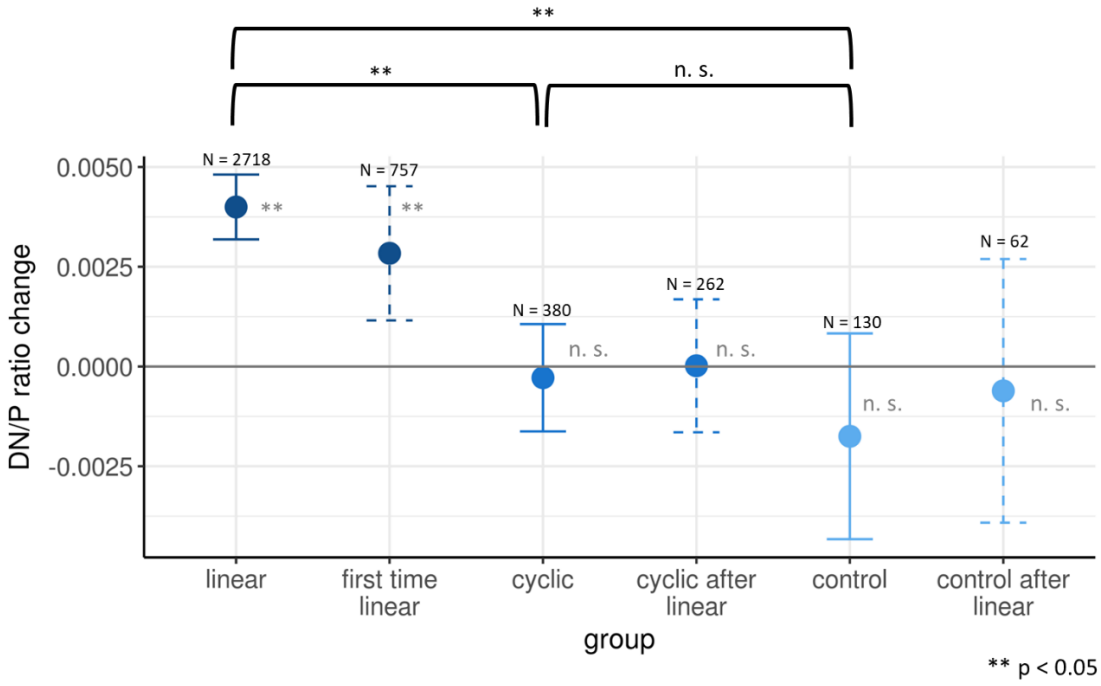

Figure 11: DN signal intensity change for different types of GBCA application.

Mean values and 95% confidence intervals of T1w signal changes within the DN are shown. One-sample t-tests (significance indicated by grey asterisks) indicate a signal increase only after application of linear gadolinium-based contrast agents (GBCA), already after the first application ("first time linear"). Two sample t-tests for the three main conditions (significance indicated by black asterisks) indicate differences in T1w signal intensity changes after application of linear GBCA compared to cyclic GBCA and no GBCA (control). One-sample t-tests in the subconditions analyses (cyclic after linear and control after linear) were not significant and thus do not suggest washout effects. First time linear, linear GBCA administered for the first time; cyclic after linear, cyclic GBCA condition follows linear GBCA condition; control after linear, control condition follows linear condition; DN/P, DN-to pons ratio; n.s., not significant; N, number of scans per analysis.

Our whole brain analyses showed significant T1w signal increases only after administration of linear GBCA. Besides the DN, we observed T1w signal increase bilaterally in the GP (Figure 12). Comparison between conditions in a two-sample t-test did not demonstrate significant differences after correction for multiple comparisons across the whole brain.

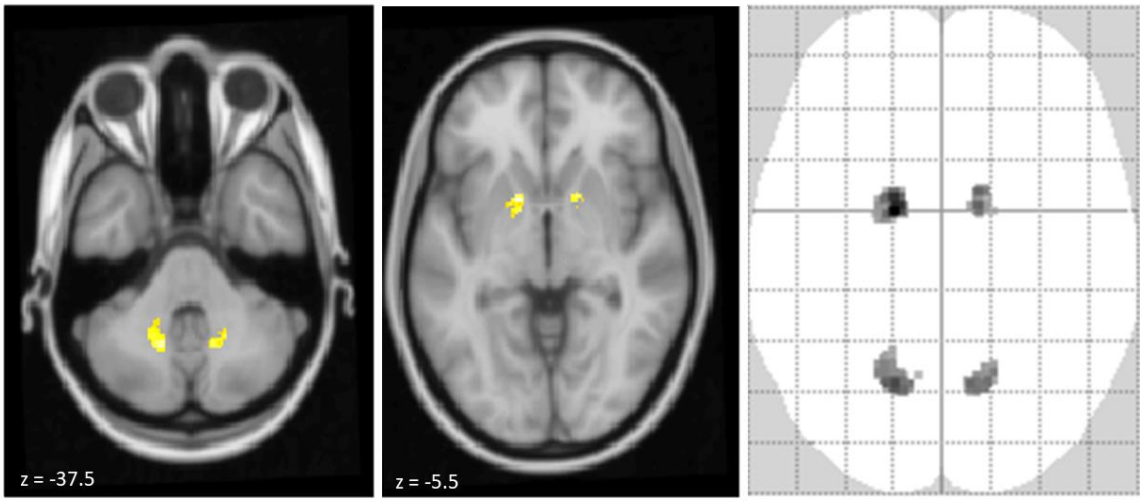

Figure 12: Whole brain analysis of T1w signal intensity change after linear GBCA application.

Whole brain voxel-based analysis of T1w signal increase after administration of the linear gadolinium-based contrast agent gadopentetic acid is shown. The one-sample t-test of difference images reveals an increase in the T1w signal not only in the DN but also in the globus pallidus (family-wise error corrected, $p < 0.05$). Significant voxels are projected on the T1w template of the software package SPM with coordinates of the z-axis (standard space of the Montreal Neurological Institute) given in the lower left corners (left, middle). Maximum intensity projection indicates that no further area was identified (right).

4 Discussion

4.1 Summary of the findings

This thesis investigated two important aspects of WM lesion evaluation by modern high-resolution 3D MRI in MS patients in two separate studies. In the first project, we provided a rationale for a WM lesion size threshold. Although WM lesions, smaller than 3 mm in diameter, are more frequent in MS patients than in control subjects, balancing sensitivity and specificity resulted in a WM lesion size threshold of 3 mm in D. In the second project, we studied T1w signal intensity changes after administration of GBCA as a surrogate for Gd accumulation in the brain of MS patients. We found signal intensity increases only after administration of linear GBCA, but not after administration of cyclic GBCA. By subgroup analysis, we demonstrated signal increase in the DN already after a single administration of linear GBCA.

4.2 Project 1: Minimal white matter lesion size threshold in MS

In this project, we aimed to provide a rationale for a minimum WM lesion size threshold of 3 mm in D to support the diagnosis of MS when using high-resolution 3D sequences from state-of-the-art 3 T scanners. We will consider the potential role of WM lesions smaller than 3 mm in D, discuss our results in more detail, acknowledge limitations of project 1 and propose how WM lesion size could be better accounted for in the future.

The finding of more small WM lesions (i.e. < 3 mm in D) in the MS group than in the CS group suggests that even small WM lesions reflect disease related structural change. Further, we confirmed the assumption that small WM lesions contribute

substantially to the count of total WM lesions (de Groot et al., 2000) in MS and CS. Yet, correlations of small WM lesion volume with disease severity (EDSS) and with thalamic volume were very weak and not consistent across scanner vendors so that the clinical importance of small WM lesions remains unclear. This ambiguity underlines the need for a rationale of a general WM lesion size threshold to outbalance sensitivity and specificity (Swanton et al., 2007) especially for high-resolution sequences at 3 T. We addressed this with a ROC analysis, revealing an optimal lesion size threshold of about 3 mm in D for both scanner vendors.

Although the results scientifically underpin the stipulated lesion size threshold, our analyses had rather low performance measures. For example, WM lesions of a D of about 3 mm (V = 0.015 ml) showed OR values of only 2.1 and 5.25, respective to both scanner sites (Figure 8). Likewise, the optimal size threshold of 3 mm in D according to our ROC analysis was accompanied by low values of sensitivity and specificity (maximum value of 0.7). Nevertheless, these values refer to the discriminative power of a single WM lesion according to its size but do not account for the occurrence of further WM lesions in the same subject. With this in mind, the low performance measures found in project 1 are not surprising, but rather fall in line with the clinical experience that interpretation of a single WM lesion is problematic.

Application of ROC analysis regarding classification of the groups of patients with RRMS and CS is not fully compatible with the clinical situation in which the diagnostic criteria were validated, namely in patients mostly presenting with a single clinical event commonly referred to as CIS. In this respect, our analysis ideally would have been applied to MRI scans of populations similar to those studied to establish the diagnostic criteria for MS, i.e. patients with CIS, followed-up for several years and classified according to the occurrence of a second demyelinating attack. However, the fact that the diagnostic criteria were validated in patients with CIS makes their

application critical in clinical situations not clearly pointing towards MS. Since no evidence for a WM lesion size threshold for the diagnostic criteria exists, we believe therefore that the determination of a WM lesion size threshold through comparison of CS and RRMS patients is a reasonable alternative. In addition, our results were robust, with a clear peak pointing towards the same WM lesion size threshold in the ROC analysis of two populations although studied at scanners from different vendors. It should be noted that our ROC analysis treated every single WM lesion of an MS patient's brain as an MS lesion, which is a rough assumption since other causes than MS for WM lesions cannot be excluded in MS patients. Further, we used an automated approach for WM lesion detection as manual segmentation of WM lesions down to a size of only two contiguous voxels is hardly feasible. Yet we acknowledge this as a limitation of project 1 as some small WM lesions were lost, and some T2-weighted hyperintensities, classified as small WM lesions, were due to image artifacts.

Finally, although this is in accordance with the current diagnostic criteria for MS (Thompson et al., 2017), we applied a single threshold to all WM lesions independent of their location. The fact that the optimal size threshold for cortical lesions seems to be smaller than 3 mm in D (Geurts et al., 2011) implies this might not be optimal. Hence, we believe that the issue of area specific WM lesion size thresholds deserves investigation in future studies.

The pathophysiological nature of MS-related small WM lesions remains unclear. The correlation between the count of small WM lesions and WM lesions larger than 3 mm in D suggests that small WM lesions may be simply a smaller version of typical WM lesions. Nevertheless, we believe that apart from the increase in spatial resolution of MRI more advanced techniques with sequences covering other aspects of MS-related pathology are necessary to understand the physiological underpinnings of small WM lesions.

Finally, we conclude that the results of project 1 support the use of the traditional WM lesion size threshold of 3 mm in D to determine WM lesion in MS – also when using state-of-the-art 3D sequences at 3 T.

4.3 Project 2: T1 intensity change after administration of gadolinium-based contrast agents

In the second project, we studied Gd retention after administration of GBCA in MS patients. Current data on correlation between GBCA administration and signal intensity change is still unclear and heterogeneous. Some in vivo human studies found T1w-signal increase after administration of the linear but not the cyclic GBCA (Eisele et al., 2016; Kanda et al., 2015b; Radbruch et al., 2017; Schlemm et al., 2017; Weberling et al., 2015), which is in line with results from our project 2. On the contrary, other groups showed signal intensity increase after administration of cyclic GBCA as well (Rossi Espagnet et al., 2017; Stojanov et al., 2016). Likewise, some (Bussi et al., 2018; McDonald et al., 2017a) but not all (Jost et al., 2016; Robert et al., 2015) animal studies demonstrated Gd deposition in the brain after repetitive administration of cyclic GBCA. Further in one post mortem study, deposits of Gd after administration of two different cyclic GBCA (gadoteridol, gadobutrol) were demonstrated (Murata et al., 2016). These differences in the reported findings between GBCA chelate types might be related to patient populations (tumor vs. MS), the use of different MR scanners or scanning protocols or different analytical approaches. With project 2, we further clarify the dynamics of linear and cyclic GBCA in patients suffering from MS. To the best of our knowledge, our analytical approach, based on difference images per GBCA administration, has not yet been used in studies on Gd deposition in the brain. We believe that, by including all available images instead of only the first and last images of each subject, we could

gather the most information from our data. Given the only small T1w signal increase after GBCA administration, averaging was necessary to detect meaningful signals. With our approach, we did not primarily average across multiple GBCA applications per subject, as done in other studies on Gd deposition in the brain (Behzadi et al., 2018; Forslin et al., 2019; Kanda et al., 2014; Kanda et al., 2015b; Radbruch et al., 2017; Radbruch et al., 2015; Schlemm et al., 2017; Weberling et al., 2015; Zivadinov et al., 2019), but across subjects per single GBCA administration. Accordingly, single subjects contributed data to more than one condition (linear, cyclic, no GBCA). This design was necessary as project 2 was done retrospectively over a period of time in which routine administration of GBCA switched from the linear GBCA gadopentetic acid (Magnevist®) to the cyclic GBCA gadoterate meglumine (Dotarem®). Additionally, it allowed us to analyze the kinetics of Gd deposition.

First, we focused on the dynamics of Gd deposition as visible in MRI. It is still under debate if several administrations are necessary to cause considerable Gd deposits in the brain. The FDA safety announcement from July 2015 states that "deposits of GBCAs remain in the brains of some patients who undergo four or more contrast MRI scans." (U.S. Food and Drug Administration, 2015). This statement is compatible with the notion that biologically meaningful non-linear effects come into play so that exceeding a certain number of administrations must be regarded as particularly critical. This is suggested by several studies on T1w signal increase after multiple GBCA administrations (Barisano et al., 2019; Kanda et al., 2015b). Alternatively, Gd deposition may be an incremental (i.e. linear) process during which the detection threshold is exceeded after a certain number of GBCA administrations, which is supported by a postmortem study on Gd accumulation after GBCA administration (McDonald et al., 2017b). Of note, the number of previous GBCA applications exerted a significant effect in our study: the more times GBCA had been administered, the higher the increase per single GBCA administration. However, this

non-linear component of the effect was very small, explaining only 0.4% of the variance of the observed T1w signal increase. Based on the assumption of linearity, we could demonstrate an increase of the T1w signal, and hence probable Gd deposition, after only one GBCA administration, challenging the idea of a safe threshold with regard to the number of GBCA administrations.

Second, we addressed the issue of a possible Gd washout by investigating subconditions ('cyclic after linear' and 'control after linear') and searched for a decrease of the T1w signal. In contrast to previous studies, we did not find any indication of a washout of Gd deposits over time (Robert et al., 2018; Smith et al., 2017) or when linear GBCA were followed by cyclic GBCA (Adin et al., 2015; Behzadi et al., 2018). Signal intensity changes of difference images from the control condition (no GBCA) also did not depend on whether linear GBCA was administered beforehand or not. We acknowledge that the results of our subcondition analyses are based on relatively low numbers of observations and our project 2 covered relatively homogeneous time intervals of 11 months. Signal changes beyond this time frame may not have been captured here.

Examining Gd deposition, the differentiation between chelated and dechelated Gd plays an important role. In an animal study by Robert and colleagues, the concentration of Gd bound to macromolecules was increased after administration of linear, but not after cyclic GBCA (Robert et al., 2018). This suggests a partial dechelation of linear GBCA in the brain tissue, followed by macromolecule binding, which causes the signal intensity increase as seen in unenhanced T1w images (Radbruch, 2018). Against this background, our results point towards a higher concentration of Gd deposits in the brain after administration of linear compared to cyclic GBCA but do not exclude Gd deposition after administration of cyclic GBCA.

No robust indication exists so far that Gd deposition after GBCA administration is accompanied by side effects (Choi & Moon, 2019; Young et al., 2019). But these

could come into play years or even decades after exposition, e.g. by accelerating neurodegeneration. Therefore, the potential risks of patients with MS, who undergo regular follow-up scans over years to monitor therapy outcomes, seems particularly relevant. The correlation between the EDSS score and number of GBCA administrations might be linked to disease severity, rather than Gd deposition. We expected this association, assuming that patients with more severe courses (including highly active patients) have more relapses and are likely to be scanned more frequently and, hence, to receive more GBCA administrations. Of note, another study investigated the sodium-related MRI signal, as a surrogate marker of potential tissue damage, in MS patients. Within areas of increased T1w signal intensities of the DN, a normal sodium signal was determined and, hence, no evidence of GBCA-related tissue damage provided (Eisele et al., 2017). In addition, there may be kinetic aspects to be considered for the evaluation of MS patients with regard to Gd deposition.

In project 2, the mean interval between two GBCA administrations (11 months) was longer than in studies on patients with tumors, usually around 3 months (Radbruch et al., 2015). We speculated that longer intervals go along with less accumulation due to longer depletion time. Yet, this does not seem to be the case. In line with four other studies (Eisele et al., 2016; Forslin et al., 2019; Schlemm et al., 2017; Zivadinov et al., 2019), patients with MS do not show different dynamics in T1w signal increases compared to tumor patients. Although human studies have not yet proven findings of CNS toxicity, based on animal studies (Muldoon & Neuwelt, 2015; Roman-Goldstein et al., 1991), the possibility of neurotoxicity of repeated doses of GBCA cannot be excluded.

Our MRI data consisted exclusively of data from a single standardized protocol including 3D FLAIR and T1w sequences. This allowed the performance of a voxel-wise whole brain analysis of T1w signal increase. In accordance with other studies applying region-of-interest analyses, we identified the DN and globus pallidus as

regions with significant signal increase, indicating most Gd deposition in these brain regions (Kanda et al., 2014; Radbruch et al., 2015; Rossi Espagnet et al., 2017; Stojanov et al., 2016). This approach has two main assumptions. First, the control region for scaling, the pons in our case, must not show the effect of interest. Some histopathological studies found Gd retention in the pons region, although in a much lower concentration compared to the DN (McDonald et al., 2015; McDonald et al., 2017b; Murata et al., 2016). Hence, deposition of lower Gd concentrations in other brain areas (than the pallidum and DN) cannot be ruled out. Second, the correction of the bias-field needs to be precise, which is not directly measurable. Yet our result of T1w signal increase within the pallidum, which is only centimeters away from the control region for scaling and reported to be a region of pronounced Gd deposition (Barisano et al., 2019; Forslin et al., 2019; Kanda et al., 2015a; Kanda et al., 2014; McDonald et al., 2015; McDonald et al., 2017b; Radbruch et al., 2015; Rossi Espagnet et al., 2017; Stojanov et al., 2016; Weberling et al., 2015), suggests that our bias correction performed well.

We acknowledge limitations of project 2. The number of observations was larger in the condition linear GBCA compared to the conditions cyclic or no GBCA. Nevertheless, the number of difference images after the first administration of linear GBCA was in the same order of magnitude as the number of images in the cyclic group and we still demonstrated a significant increase of the T1w signal. Moreover, the number of 380 difference images after cyclic GBCA was still comparably high. We also acknowledge that the results of our subcondition analyses are based on relatively low numbers of observations; nevertheless, in none of the subconditions, we observed any trend pointing towards the hypothesized effect of GBCA reversibility.

Finally, we conclude that administration of linear GBCA leads to Gd deposition in the GP and, already after a single administration, in the DN. Our findings are in

line other data which have led to the latest announcements of the European Medicines Agency (European Medicines Agency, 2017). Currently, cyclic GBCA are still permitted for imaging of the CNS whilst the use of linear GBCA has been restricted. The Consortium of MS Centers still regards GBCA as indispensable for diagnostic purposes but as optional for follow-up investigations (Traboulsee et al., 2016).

4.4 Conclusion and outlook

This thesis investigated two important aspects of WM lesion evaluation by state-of-the-art MRI in MS. In project 1, we provided a rationale for a minimal WM lesion size threshold. We found that the traditionally stipulated threshold of 3 mm in D is a reasonable choice also when applying 3D sequences at 3T.

To the best of our knowledge, so far, no study has investigated a meaningful minimal WM lesion size. The advantage of such a parameter would be a more sensitive and possibly earlier diagnosis of MS. Studies suggest early diagnosis would lead to better long-term disease outcome due to faster initiation of therapy with disease modifying drugs (Freedman et al., 2014; Giovannoni et al., 2016). In people with CIS, who were treated with a disease modifying therapy, the risk for a second relapse and thus conversion to clinically definite MS, was reduced compared to placebo control groups and MRI outcomes such as brain atrophy rates or development of new lesions were improved (Comi et al., 2009; Filippi et al., 2004; Jacobs et al., 2000; Miller et al., 2014). These insights have led to a drastic decrease of time to diagnosis from 7.2 to 0.6 years after the first symptoms of MS (Marrie et al., 2005). A tension has been created between the benefits of an early diagnosis and the risks of misdiagnosis (Solomon & Corboy, 2017). This is especially relevant against the background of fast technological progress, making the most subtle deviations visible in MRI. Until a

highly specific MS biomarker is found, it could be helpful to improve existing biomarkers (such as WM lesions) and make the diagnosis as standardized and scientifically validated as possible, for example by defining a scientifically evident minimal WM lesion size threshold.

Regarding conventional T2w sequences, future work should concentrate on criteria, based on size and perhaps shape that are specific for different diagnostic areas of the CNS. For further improvement of sensitivity and specificity, the use of more advanced sequences, covering typical features of MS-related pathology such as the central vein sign, seems necessary.

Besides the early diagnosis, the safety of MS patients during the diagnostic process is an important issue. Despite many studies, showing Gd deposition in the brain after GBCA administration, FDA for example still allows administration of linear GBCA and most studies stipulate deposition only after a certain safe threshold, a certain number of administrations (U.S. Food and Drug Administration, 2015).

In project 2, we found indications of Gd deposition in the brain, only after linear GBCA, which could be detected even after a single administration, whilst we did not find any indication of Gd deposition in the brain after the administration of cyclic GBCA. Our findings lend support to recent decisions of the European Medicines Agency, which suspended linear GBCA for the primary use in CNS imaging (European Medicines Agency, 2017). Whether alternative contrasts agents, like manganese-based and iron-based complexes which are currently under investigation, are safer than GBCA, remains to be determined. De facto, there are only few animal studies indicating potential side effects of Gd deposition in the brain. Nevertheless, adverse health reactions cannot be ruled out and more research is needed. Alternatively, the use of GBCA could be largely spared. In MS, recent approaches to precisely compare individual follow-up images without the help of GBCA are promising and suggest that GBCA are dispensable for most MRI

investigations to monitor the course of the disease (Eichinger et al., 2019)). Further, more advanced MRI sequences seem to be able to determine the integrity of the blood brain barrier without GBCA (Falk Delgado et al., 2019).

This thesis emphasizes that standardized and scientifically sound MR protocols are indispensable to further improve the quality of MR diagnostic processes, make them safer and more objective.

5 Acknowledgements

First and foremost, I would like to express my sincere gratitude to my supervisor Mark Mühlau for the great mentorship during my Ph.D study and related research, for his patience, motivation and immense knowledge.

Besides my advisor, I would like to thank my thesis committee: Markus Ploner and Christian Sorg for their insightful comments and encouragement. It has been a privilege to work with you all.

I am thankful to the Department of Neurology and all its member`s staff, especially Achim Berthele and Bernhard Hemmer for your support and fruitful cooperation.

My work would not have been possible without the great help and courtesy of the Department of Neuroradiology at the Klinikum rechts der Isar, particularly Jan Kirschke and Claus Zimmer. Thanks to Daniel Fröbel for the great technical support.

I kindly thank my collaborators in the first thesis project, the research group around Sergui Groppa from the department of neurology, led by Frauke Zipp at Johannes-Guttenberg University of Mainz.

Special thanks go to Matthias Bussas, you were my number one programming teacher, my supporter in good and hard times and my contact person for all kind of professional and private issues.

I am very grateful for my warm, open and inspiring working environment in the past 4 years. Thanks to Christina Engl, Viola Pongratz, Laura Bok, Elisabeth May, Moritz Nickel, Vanessa Hohn, Cristina Avila and Henrik Heitmann – you are not only the best colleagues ever, but really good friends. Additional thanks to all past and current members of the TUM-NIC, it was a pleasure working among you!

Finally, very special thanks to Son Ta Dinh for your numerous neck massages, your unshakeable patience, your pragmatism and for knowing always how to cheer me up.

This thesis is dedicated to my family and all the people who helped me to be where I am right now.

6 References

Absinta, M., Rocca, M. A., & Filippi, M. (2011). Dentate nucleus T1 hyperintensity in multiple sclerosis. *AJNR Am J Neuroradiol, 32*(6), E120-121.

Adin, Kleinberg, L., Vaidya, D., Zan, E., Mirbagheri, S., & Yousem, D. M. (2015). Hyperintense Dentate Nuclei on T1-Weighted MRI: Relation to Repeat Gadolinium Administration. *American Journal of Neuroradiology, 36*(10), 1859-1865.

Albrecht, D. S., Granziera, C., Hooker, J. M., & Loggia, M. L. (2016). In Vivo Imaging of Human Neuroinflammation. *ACS Chem Neurosci, 7*(4), 470-483.

Ali, E. N., & Buckle, G. J. (2009). Neuroimaging in multiple sclerosis. *Neurol Clin, 27*(1), 203-219, ix.

Andlauer, T. F., Buck, D., Antony, G., Bayas, A., Bechmann, L., Berthele, A., Chan, A., Gasperi, C., Gold, R., Graetz, C., Haas, J., Hecker, M., Infante-Duarte, C., Knop, M., Kumpfel, T., Limmroth, V., Linker, R. A., Loleit, V., Luessi, F., Meuth, S. G., Muhlau, M., Nischwitz, S., Paul, F., Putz, M., Ruck, T., Salmen, A., Stangel, M., Stellmann, J. P., Sturner, K. H., Tackenberg, B., Then Bergh, F., Tumani, H., Warnke, C., Weber, F., Wiendl, H., Wildemann, B., Zettl, U. K., Ziemann, U., Zipp, F., Arloth, J., Weber, P., Radivojkov-Blagojevic, M., Scheinhardt, M. O., Dankowski, T., Bettecken, T., Lichtner, P., Czamara, D., Carrillo-Roa, T., Binder, E. B., Berger, K., Bertram, L., Franke, A., Gieger, C., Herms, S., Homuth, G., Ising, M., Jockel, K. H., Kacprowski, T., Kloiber, S., Laudes, M., Lieb, W., Lill, C. M., Lucae, S., Meitinger, T., Moebus, S., Muller-Nurasyid, M., Nothen, M. M., Petersmann, A., Rawal, R., Schminke, U., Strauch, K., Volzke, H., Waldenberger, M., Wellmann, J., Porcu, E., Mulas, A., Pitzalis, M., Sidore, C., Zara, I., Cucca, F., Zoledziewska, M., Ziegler, A., Hemmer, B., & Muller-Myhsok, B. (2016). Novel multiple sclerosis susceptibility loci implicated in epigenetic regulation. *Sci Adv, 2*(6), e1501678.

Ascherio, A., & Munger, K. L. (2007a). Environmental risk factors for multiple sclerosis. Part I: the role of infection. *Ann Neurol, 61*(4), 288-299.

Ascherio, A., & Munger, K. L. (2007b). Environmental risk factors for multiple sclerosis. Part II: Noninfectious factors. *Ann Neurol, 61*(6), 504-513.

Ashburner, J., & Friston, K. J. (2007). Segmentation. In K. J. Friston, J. Ashburner, S. Kiebel, T. E. Nichols, & W. Penny (Eds.), *Statistical Parametric Mapping: The Analysis of Functional Brain Images* (pp. 81-91): Elsevier.

Barisano, G., Bigjahan, B., Metting, S., Cen, S., Amezcua, L., Lerner, A., Toga, A. W., & Law, M. (2019). Signal Hyperintensity on Unenhanced T1-Weighted

Brain and Cervical Spinal Cord MR Images after Multiple Doses of Linear Gadolinium-Based Contrast Agent. *AJNR Am J Neuroradiol, 40*(8), 1274-1281.

Barkhof, F., Filippi, M., Miller, D. H., Scheltens, P., Campi, A., Polman, C. H., Comi, G., Ader, H. J., Losseff, N., & Valk, J. (1997). Comparison of MRI criteria at first presentation to predict conversion to clinically definite multiple sclerosis. *Brain, 120 (Pt 11)*(11), 2059-2069.

Battaglini, M., Jenkinson, M., & De Stefano, N. (2012). Evaluating and reducing the impact of white matter lesions on brain volume measurements. *Hum Brain Mapp, 33*(9), 2062-2071.

Behzadi, A. H., Farooq, Z., Zhao, Y., Shih, G., & Prince, M. R. (2018). Dentate Nucleus Signal Intensity Decrease on T1-weighted MR Images after Switching from Gadopentetate Dimeglumine to Gadobutrol. *Radiology, 287*(3), 816-823.

Belbasis, L., Bellou, V., Evangelou, E., Ioannidis, J. P., & Tzoulaki, I. (2015). Environmental risk factors and multiple sclerosis: an umbrella review of systematic reviews and meta-analyses. *Lancet Neurol, 14*(3), 263-273.

Bellin, M. F., & Van Der Molen, A. J. (2008). Extracellular gadolinium-based contrast media: an overview. *Eur J Radiol, 66*(2), 160-167.

Bink, A., Schmitt, M., Gaa, J., Mugler, J. P., 3rd, Lanfermann, H., & Zanella, F. E. (2006). Detection of lesions in multiple sclerosis by 2D FLAIR and single-slab 3D FLAIR sequences at 3.0 T: initial results. *Eur Radiol, 16*(5), 1104-1110.

Bo, L., Vedeler, C. A., Nyland, H. I., Trapp, B. D., & Mork, S. J. (2003). Subpial demyelination in the cerebral cortex of multiple sclerosis patients. *J Neuropathol Exp Neurol, 62*(7), 723-732.

Bot, J., Barkhof, F., Lycklama, G. J., van Schaardenburg, D., Voskuyl, A. E., Ader, H., Pijnenburg, J., Polman, C., Uitdehaag, B., Vermeulen, E., & Castelijns, J. A. (2002). Differentiation of Multiple Sclerosis from Other Inflammatory Disorders and Cerebrovascular Disease: Value of Spinal MR Imaging. *Radiology, 223*(1), 46-56.

Bravo, Á. P., Hernández, J. J. S., Sanz, L. I., Cáceres, I. A. d., José, J. L. C. S., & Gandariaga, B. G.-C. (2014). A comparative MRI study for white matter hyperintensities detection: 2D-FLAIR, FSE PD 2D, 3D-FLAIR and FLAIR MIP. *The British Journal of Radiology, 87*(1035), 20130360.

Brett, M., Leff, A. P., Rorden, C., & Ashburner, J. (2001). Spatial normalization of brain images with focal lesions using cost function masking. *NeuroImage, 14*(2), 486-500.

Brex, P. A., Ciccarelli, O., O'Riordan, J. I., Sailer, M., Thompson, A. J., & Miller, D. H. (2002). A longitudinal study of abnormalities on MRI and disability from multiple sclerosis. *N Engl J Med, 346*(3), 158-164.

Brickman, A. M., Zahodne, L. B., Guzman, V. A., Narkhede, A., Meier, I. B., Griffith, E. Y., Provenzano, F. A., Schupf, N., Manly, J. J., Stern, Y., Luchsinger, J. A., & Mayeux, R. (2015). Reconsidering harbingers of dementia: progression of parietal lobe white matter hyperintensities predicts Alzheimer's disease incidence. *Neurobiol Aging, 36*(1), 27-32.

Browne, P., Chandraratna, D., Angood, C., Tremlett, H., Baker, C., Taylor, B. V., & Thompson, A. J. (2014). Atlas of multiple sclerosis 2013: a growing global problem with widespread inequity. *Neurology, 83*, 1022-1024.

Brownlee, W. J., Hardy, T. A., Fazekas, F., & Miller, D. H. (2017). Diagnosis of multiple sclerosis: progress and challenges. *Lancet, 389*(10076), 1336-1346.

Bruck, W., Bitsch, A., Kolenda, H., Bruck, Y., Stiefel, M., & Lassmann, H. (1997). Inflammatory central nervous system demyelination: correlation of magnetic resonance imaging findings with lesion pathology. *Ann Neurol, 42*(5), 783-793.

Bussi, S., Coppo, A., Botteron, C., Fraimbault, V., Fanizzi, A., De Laurentiis, E., Colombo Serra, S., Kirchin, M. A., Tedoldi, F., & Maisano, F. (2018). Differences in gadolinium retention after repeated injections of macrocyclic MR contrast agents to rats. *J Magn Reson Imaging, 47*(3), 746-752.

Carassiti, D., Altmann, D. R., Petrova, N., Pakkenberg, B., Scaravilli, F., & Schmierer, K. (2018). Neuronal loss, demyelination and volume change in the multiple sclerosis neocortex. *Neuropathology and Applied Neurobiology, 44*(4), 377-390.

Chagla, G. H., Busse, R. F., Sydnor, R., Rowley, H. A., & Turski, P. A. (2008). Three-dimensional fluid attenuated inversion recovery imaging with isotropic resolution and nonselective adiabatic inversion provides improved three-dimensional visualization and cerebrospinal fluid suppression compared to two-dimensional flair at 3 tesla. *Invest Radiol, 43*(8), 547-551.

Chard, D. T., Jackson, J. S., Miller, D. H., & Wheeler-Kingshott, C. A. (2010). Reducing the impact of white matter lesions on automated measures of brain gray and white matter volumes. *J Magn Reson Imaging, 32*(1), 223-228.

Choi, J. W., & Moon, W. J. (2019). Gadolinium Deposition in the Brain: Current Updates. *Korean J Radiol, 20*(1), 134-147.

Chung, K. K., Altmann, D., Barkhof, F., Miszkiel, K., Brex, P. A., O'Riordan, J., Ebner, M., Prados, F., Cardoso, M. J., Vercauteren, T., Ourselin, S., Thompson, A., Ciccarelli, O., & Chard, D. T. (2020). A 30-Year Clinical and Magnetic

Resonance Imaging Observational Study of Multiple Sclerosis and Clinically Isolated Syndromes. *Ann Neurol, 87*(1), 63-74.

Cifelli, A., Arridge, M., Jezzard, P., Esiri, M. M., Palace, J., & Matthews, P. M. (2002). Thalamic neurodegeneration in multiple sclerosis. *Ann Neurol, 52*(5), 650-653.

Comi, G., Martinelli, V., Rodegher, M., Moiola, L., Bajenaru, O., Carra, A., Elovaara, I., Fazekas, F., Hartung, H. P., Hillert, J., King, J., Komoly, S., Lubetzki, C., Montalban, X., Myhr, K. M., Ravnborg, M., Rieckmann, P., Wynn, D., Young, C., Filippi, M., & Pre, C. s. g. (2009). Effect of glatiramer acetate on conversion to clinically definite multiple sclerosis in patients with clinically isolated syndrome (PreCISe study): a randomised, double-blind, placebo-controlled trial. *Lancet, 374*(9700), 1503-1511.

Compston, A., & Coles, A. (2008). Multiple sclerosis. *Lancet, 372*(9648), 1502-1517.

Cotton, F., Weiner, H. L., Jolesz, F. A., & Guttmann, C. R. (2003). MRI contrast uptake in new lesions in relapsing-remitting MS followed at weekly intervals. *Neurology, 60*(4), 640-646.

De Coene, B., Hajnal, J. V., Gatehouse, P., Longmore, D. B., White, S. J., Oatridge, A., Pennock, J. M., Young, I. R., & Bydder, G. M. (1992). MR of the brain using fluid-attenuated inversion recovery (FLAIR) pulse sequences. *American Journal of Neuroradiology, 13*(6), 1555-1564.

de Groot, J. C., de Leeuw, F. E., Oudkerk, M., van Gijn, J., Hofman, A., Jolles, J., & Breteler, M. M. (2000). Cerebral white matter lesions and cognitive function: the Rotterdam Scan Study. *Ann Neurol, 47*(2), 145-151.

de Leeuw, F. E., de Groot, J. C., Oudkerk, M., Witteman, J. C., Hofman, A., van Gijn, J., & Breteler, M. M. (2002). Hypertension and cerebral white matter lesions in a prospective cohort study. *Brain, 125*(Pt 4), 765-772.

Diez, Y., Oliver, A., Cabezas, M., Valverde, S., Marti, R., Vilanova, J. C., Ramio-Torrenta, L., Rovira, A., & Llado, X. (2014). Intensity based methods for brain MRI longitudinal registration. A study on multiple sclerosis patients. *Neuroinformatics, 12*(3), 365-379.

Disanto, G., Morahan, J. M., Barnett, M. H., Giovannoni, G., & Ramagopalan, S. V. (2012). The evidence for a role of B cells in multiple sclerosis. *Neurology, 78*(11), 823-832.

Ebers, G. C., Sadovnick, A. D., Dyment, D. A., Yee, I. M., Willer, C. J., & Risch, N. (2004). Parent-of-origin effect in multiple sclerosis: observations in half-siblings. *Lancet, 363*(9423), 1773-1774.

Egger, C., Opfer, R., Wang, C., Kepp, T., Sormani, M. P., Spies, L., Barnett, M., & Schippling, S. (2017). MRI FLAIR lesion segmentation in multiple sclerosis: Does automated segmentation hold up with manual annotation? *NeuroImage: Clinical, 13*, 264-270.

Eichinger, P., Schon, S., Pongratz, V., Wiestler, H., Zhang, H., Bussas, M., Hoshi, M. M., Kirschke, J., Berthele, A., Zimmer, C., Hemmer, B., Muhlau, M., & Wiestler, B. (2019). Accuracy of Unenhanced MRI in the Detection of New Brain Lesions in Multiple Sclerosis. *Radiology, 291*(2), 429-435.

Eisele, P., Alonso, A., Szabo, K., Ebert, A., Ong, M., Schoenberg, S. O., & Gass, A. (2016). Lack of increased signal intensity in the dentate nucleus after repeated administration of a macrocyclic contrast agent in multiple sclerosis: An observational study. *Medicine (Baltimore), 95*(39), e4624.

Eisele, P., Konstandin, S., Szabo, K., Ong, M., Zollner, F., Schad, L. R., Schoenberg, S. O., & Gass, A. (2017). Sodium MRI of T1 High Signal Intensity in the Dentate Nucleus due to Gadolinium Deposition in Multiple Sclerosis. *J Neuroimaging, 27*(4), 372-375.

Errante, Y., Cirimele, V., Mallio, C. A., Di Lazzaro, V., Zobel, B. B., & Quattrocchi, C. C. (2014). Progressive increase of T1 signal intensity of the dentate nucleus on unenhanced magnetic resonance images is associated with cumulative doses of intravenously administered gadodiamide in patients with normal renal function, suggesting dechelation. *Invest Radiol, 49*(10), 685-690.

European Medicines Agency. (2017). EMA's final opinion confirms restrictions on use of linear gadolinium agents in body scans.

Falk Delgado, A., Van Westen, D., Nilsson, M., Knutsson, L., Sundgren, P. C., Larsson, E. M., & Falk Delgado, A. (2019). Diagnostic value of alternative techniques to gadolinium-based contrast agents in MR neuroimaging-a comprehensive overview. *Insights Imaging, 10*(1), 84.

Fazekas, F., Barkhof, F., Filippi, M., Grossman, R. I., Li, D. K., McDonald, W. I., McFarland, H. F., Paty, D. W., Simon, J. H., Wolinsky, J. S., & Miller, D. H. (1999). The contribution of magnetic resonance imaging to the diagnosis of multiple sclerosis. *Neurology, 53*(3), 448-456.

Filippi, M., Brück, W., Chard, D., Fazekas, F., Geurts, J. J. G., Enzinger, C., Hametner, S., Kuhlmann, T., Preziosa, P., Rovira, À., Schmierer, K., Stadelmann, C., & Rocca, M. A. (2019). Association between pathological and MRI findings in multiple sclerosis. *The Lancet Neurology, 18*(2), 198-210.

Filippi, M., Rocca, M. A., Barkhof, F., Brück, W., Chen, J. T., Comi, G., DeLuca, G., De Stefano, N., Erickson, B. J., Evangelou, N., Fazekas, F., Geurts, J. J. G.,

Lucchinetti, C., Miller, D. H., Pelletier, D., Popescu, B. F. G., & Lassmann, H. (2012). Association between pathological and MRI findings in multiple sclerosis. *The Lancet Neurology, 11*(4), 349-360.

Filippi, M., Rocca, M. A., Ciccarelli, O., De Stefano, N., Evangelou, N., Kappos, L., Rovira, A., Sastre-Garriga, J., Tintorè, M., Frederiksen, J. L., Gasperini, C., Palace, J., Reich, D. S., Banwell, B., Montalban, X., & Barkhof, F. (2016). MRI criteria for the diagnosis of multiple sclerosis: MAGNIMS consensus guidelines. *The Lancet Neurology, 15*(3), 292-303.

Filippi, M., Rovaris, M., Bastianello, S., Gasperini, C., Origgi, D., Reganati, P., Pozzilli, C., & Comi, G. (1999). A comparison of the sensitivity of monthly unenhanced and enhanced MRI techniques in detecting new multiple sclerosis lesions. *Journal of Neurology, 246*(2), 97-106.

Filippi, M., Rovaris, M., Inglese, M., Barkhof, F., De Stefano, N., Smith, S., Comi, G., & Grp, E. S. (2004). Interferon beta-1a for brain tissue loss in patients at presentation with syndromes suggestive of multiple sclerosis: a randomised, double-blind, placebo-controlled trial. *Lancet, 364*(9444), 1489-1496.

Filippi, M., Yousry, T., Baratti, C., Horsfield, M. A., Mammi, S., Becker, C., Voltz, R., Spuler, S., Campi, A., Reiser, M. F., & Comi, G. (1996). Quantitative assessment of MRI lesion load in multiple sclerosis. A comparison of conventional spin-echo with fast fluid-attenuated inversion recovery. *Brain, 119 (Pt 4)*(4), 1349-1355.

Fisniku, L. K., Brex, P. A., Altmann, D. R., Miszkiel, K. A., Benton, C. E., Lanyon, R., Thompson, A. J., & Miller, D. H. (2008). Disability and T2 MRI lesions: a 20-year follow-up of patients with relapse onset of multiple sclerosis. *Brain, 131*(3), 808-817.

Florkowski, C. M. (2008). Sensitivity, specificity, receiver-operating characteristic (ROC) curves and likelihood ratios: communicating the performance of diagnostic tests. *Clin Biochem Rev, 29 Suppl 1*(Suppl 1), S83-87.

Forslin, Y., Martola, J., Bergendal, A., Fredrikson, S., Wiberg, M. K., & Granberg, T. (2019). Gadolinium Retention in the Brain: An MRI Relaxometry Study of Linear and Macrocyclic Gadolinium-Based Contrast Agents in Multiple Sclerosis. *AJNR Am J Neuroradiol, 40*(8), 1265-1273.

Freedman, M. S., Comi, G., De Stefano, N., Barkhof, F., Polman, C. H., Uitdehaag, B. M., Lehr, L., Stubinski, B., & Kappos, L. (2014). Moving toward earlier treatment of multiple sclerosis: Findings from a decade of clinical trials and implications for clinical practice. *Mult Scler Relat Disord, 3*(2), 147-155.

Friston, K. J., Ashburner, J., Frith, C. D., Poline, J. B., Heather, J. D., & Frackowiak, R. S. J. (1995). Spatial registration and normalization of images. *Human Brain Mapping, 3*(3), 165-189.

Frohman, E. M., Racke, M. K., & Raine, C. S. (2006). Multiple sclerosis--the plaque and its pathogenesis. *N Engl J Med, 354*(9), 942-955.

Gaitan, M. I., Shea, C. D., Evangelou, I. E., Stone, R. D., Fenton, K. M., Bielekova, B., Massacesi, L., & Reich, D. S. (2011). Evolution of the blood-brain barrier in newly forming multiple sclerosis lesions. *Ann Neurol, 70*(1), 22-29.

Geurts, J. J., Roosendaal, S. D., Calabrese, M., Ciccarelli, O., Agosta, F., Chard, D. T., Gass, A., Huerga, E., Moraal, B., Pareto, D., Rocca, M. A., Wattjes, M. P., Yousry, T. A., Uitdehaag, B. M., Barkhof, F., & Group, M. S. (2011). Consensus recommendations for MS cortical lesion scoring using double inversion recovery MRI. *Neurology, 76*(5), 418-424.

Gilmore, C. P., Donaldson, I., Bo, L., Owens, T., Lowe, J., & Evangelou, N. (2009). Regional variations in the extent and pattern of grey matter demyelination in multiple sclerosis: a comparison between the cerebral cortex, cerebellar cortex, deep grey matter nuclei and the spinal cord. *J Neurol Neurosurg Psychiatry, 80*(2), 182-187.

Giovannoni, G., Butzkueven, H., Dhib-Jalbut, S., Hobart, J., Kobelt, G., Pepper, G., Sormani, M. P., Thalheim, C., Traboulsee, A., & Vollmer, T. (2016). Brain health: time matters in multiple sclerosis. *Mult Scler Relat Disord, 9 Suppl 1*, S5-S48.

Gold, R., Hanschke, S., Hemmer, B., & Wiendl, H. (2012). Diagnose und Therapie der Multiplen Sklerose. In *Leitlinien für Diagnostik und Therapie in der Neurologie* (Vol. 5, pp. 430-475).

Grahl, S., Bussas, M., Pongratz, V., Kirschke, J. S., Zimmer, C., Berthele, A., Hemmer, B., & Muhlau, M. (2020). T1-Weighted Intensity Increase After a Single Administration of a Linear Gadolinium-Based Contrast Agent in Multiple Sclerosis. *Clin Neuroradiol*.

Grahl, S., Pongratz, V., Schmidt, P., Engl, C., Bussas, M., Radetz, A., Gonzalez-Escamilla, G., Groppa, S., Zipp, F., Lukas, C., Kirschke, J., Zimmer, C., Hoshi, M., Berthele, A., Hemmer, B., & Muhlau, M. (2019). Evidence for a white matter lesion size threshold to support the diagnosis of relapsing remitting multiple sclerosis. *Mult Scler Relat Disord, 29*, 124-129.

Grobner, T. (2006). Gadolinium--a specific trigger for the development of nephrogenic fibrosing dermopathy and nephrogenic systemic fibrosis? *Nephrol Dial Transplant, 21*(4), 1104-1108.

Hagens, M. H. J., Burggraaff, J., Kilsdonk, I. D., de Vos, M. L., Cawley, N., Sbardella, E., Andelova, M., Amann, M., Lieb, J. M., Pantano, P., Lissenberg-Witte, B. I., Killestein, J., Oreja-Guevara, C., Ciccarelli, O., Gasperini, C., Lukas, C., Wattjes, M. P., Barkhof, F., & Group, M. S. (2018). Three-Tesla MRI does not improve the diagnosis of multiple sclerosis: A multicenter study. *Neurology, 91*(3), e249-e257.

Hauser, S. L., Bar-Or, A., Comi, G., Giovannoni, G., Hartung, H. P., Hemmer, B., Lublin, F., Montalban, X., Rammohan, K. W., Selmaj, K., Traboulsee, A., Wolinsky, J. S., Arnold, D. L., Klingelschmitt, G., Masterman, D., Fontoura, P., Belachew, S., Chin, P., Mairon, N., Garren, H., Kappos, L., Opera, I., & Investigators, O. I. C. (2017). Ocrelizumab versus Interferon Beta-1a in Relapsing Multiple Sclerosis. *N Engl J Med, 376*(3), 221-234.

Herranz, E., Gianni, C., Louapre, C., Treaba, C. A., Govindarajan, S. T., Ouellette, R., Loggia, M. L., Sloane, J. A., Madigan, N., Izquierdo-Garcia, D., Ward, N., Mangeat, G., Granberg, T., Klawiter, E. C., Catana, C., Hooker, J. M., Taylor, N., Ionete, C., Kinkel, R. P., & Mainero, C. (2016). Neuroinflammatory component of gray matter pathology in multiple sclerosis. *Ann Neurol, 80*(5), 776-790.

Hu, X. Y., Rajendran, L., Lapointe, E., Tam, R., Li, D., Traboulsee, A., & Rauscher, A. (2019). Three-dimensional MRI sequences in MS diagnosis and research. *Mult Scler, 25*(13), 1700-1709.

International Multiple Sclerosis Genetics Consortium. (2019). Multiple sclerosis genomic map implicates peripheral immune cells and microglia in susceptibility. *Science, 365*(6460).

Jacobs, L. D., Beck, R. W., Simon, J. H., Kinkel, R. P., Brownscheidle, C. M., Murray, T. J., Simonian, N. A., Slasor, P. J., & Sandrock, A. W. (2000). Intramuscular interferon beta-1a therapy initiated during a first demyelinating event in multiple sclerosis. CHAMPS Study Group. *N Engl J Med, 343*(13), 898-904.

Jersild, C., Svejgaard, A., & Fog, T. (1972). HL-A ANTIGENS AND MULTIPLE SCLEROSIS. *The Lancet, 299*(7762), 1240-1241.

Jost, G., Lenhard, D. C., Sieber, M. A., Lohrke, J., Frenzel, T., & Pietsch, H. (2016). Signal Increase on Unenhanced T1-Weighted Images in the Rat Brain After Repeated, Extended Doses of Gadolinium-Based Contrast Agents: Comparison of Linear and Macrocyclic Agents. *Invest Radiol, 51*(2), 83-89.

Kanda, T., Fukusato, T., Matsuda, M., Toyoda, K., Oba, H., Kotoku, J., Haruyama, T., Kitajima, K., & Furui, S. (2015a). Gadolinium-based Contrast Agent Accumulates in the Brain Even in Subjects without Severe Renal

Dysfunction: Evaluation of Autopsy Brain Specimens with Inductively Coupled Plasma Mass Spectroscopy. *Radiology, 276*(1), 228-232.

Kanda, T., Ishii, K., Kawaguchi, H., Kitajima, K., & Takenaka, D. (2014). High signal intensity in the dentate nucleus and globus pallidus on unenhanced T1-weighted MR images: relationship with increasing cumulative dose of a gadolinium-based contrast material. *Radiology, 270*(3), 834-841.

Kanda, T., Nakai, Y., Hagiwara, A., Oba, H., Toyoda, K., & Furui, S. (2017). Distribution and chemical forms of gadolinium in the brain: a review. *The British Journal of Radiology, 90*(1079), 20170115.

Kanda, T., Osawa, M., Oba, H., Toyoda, K., Kotoku, J., Haruyama, T., Takeshita, K., & Furui, S. (2015b). High Signal Intensity in Dentate Nucleus on Unenhanced T1-weighted MR Images: Association with Linear versus Macrocyclic Gadolinium Chelate Administration. *Radiology, 275*(3), 803-809.

Kappos, L., Li, D., Calabresi, P. A., O'Connor, P., Bar-Or, A., Barkhof, F., Yin, M., Leppert, D., Glanzman, R., Tinbergen, J., & Hauser, S. L. (2011). Ocrelizumab in relapsing-remitting multiple sclerosis: a phase 2, randomised, placebo-controlled, multicentre trial. *Lancet, 378*(9805), 1779-1787.

Kasahara, S., Miki, Y., Kanagaki, M., Yamamoto, A., Mori, N., Sawada, T., Taoka, T., Okada, T., & Togashi, K. (2011). Hyperintense Dentate Nucleus on Unenhanced T1-weighted MR Images Is Associated with a History of Brain Irradiation. *Radiology, 258*(1), 222-228.

Kasper, L. H., & Shoemaker, J. (2010). Multiple sclerosis immunology. *The healthy immune system vs the MS immune system, 74*(1 Supplement 1), S2-S8.

Kearney, H., Altmann, D. R., Samson, R. S., Yiannakas, M. C., Wheeler-Kingshott, C. A., Ciccarelli, O., & Miller, D. H. (2015). Cervical cord lesion load is associated with disability independently from atrophy in MS. *Neurology, 84*(4), 367-373.

Koch-Henriksen, N., & Sørensen, P. S. (2010). The changing demographic pattern of multiple sclerosis epidemiology. *The Lancet Neurology, 9*(5), 520-532.

Kurtzke, J. F. (1983). Rating neurologic impairment in multiple sclerosis: an expanded disability status scale (EDSS). *Neurology, 33*(11), 1444-1452.

Kutzelnigg, A., Lucchinetti, C. F., Stadelmann, C., Bruck, W., Rauschka, H., Bergmann, M., Schmidbauer, M., Parisi, J. E., & Lassmann, H. (2005). Cortical demyelination and diffuse white matter injury in multiple sclerosis. *Brain, 128*(Pt 11), 2705-2712.

Lagumersindez-Denis, N., Wrzos, C., Mack, M., Winkler, A., van der Meer, F., Reinert, M. C., Hollasch, H., Flach, A., Bruhl, H., Cullen, E., Schlumbohm, C., Fuchs, E., Linington, C., Barrantes-Freer, A., Metz, I., Wegner, C., Liebetanz, D., Prinz, M., Bruck, W., Stadelmann, C., & Nessler, S. (2017). Differential contribution of immune effector mechanisms to cortical demyelination in multiple sclerosis. *Acta Neuropathol, 134*(1), 15-34.

Lassmann, H. (2011). A dynamic view of the blood-brain barrier in active multiple sclerosis lesions. *Ann Neurol, 70*(1), 1-2.

Leray, E., Moreau, T., Fromont, A., & Edan, G. (2016). Epidemiology of multiple sclerosis. *Rev Neurol (Paris), 172*(1), 3-13.

Loria, K. (2016). Technology Trends: MRI Time to Upgrade? — Considerations for the Move From 1.5T to 3T. *Radiology Today, 17*(2).

Magliozzi, R., Howell, O. W., Reeves, C., Roncaroli, F., Nicholas, R., Serafini, B., Aloisi, F., & Reynolds, R. (2010). A Gradient of neuronal loss and meningeal inflammation in multiple sclerosis. *Ann Neurol, 68*(4), 477-493.

Manjón, J. V. (2017). MRI Preprocessing. In L. Martí-Bonmatí & A. Alberich-Bayarri (Eds.), *Imaging Biomarkers: Development and Clinical Integration* (pp. 53-63). Cham: Springer International Publishing.

Marckmann, P., Skov, L., Rossen, K., Dupont, A., Damholt, M. B., Heaf, J. G., & Thomsen, H. S. (2006). Nephrogenic systemic fibrosis: suspected causative role of gadodiamide used for contrast-enhanced magnetic resonance imaging. *J Am Soc Nephrol, 17*(9), 2359-2362.

Marrie, R. A., Cutter, G., Tyry, T., Hadjimichael, O., Campagnolo, D., & Vollmer, T. (2005). Changes in the ascertainment of multiple sclerosis. *Neurology, 65*(7), 1066-1070.

McDonald, R. J., McDonald, J. S., Dai, D., Schroeder, D., Jentoft, M. E., Murray, D. L., Kadirvel, R., Eckel, L. J., & Kallmes, D. F. (2017a). Comparison of Gadolinium Concentrations within Multiple Rat Organs after Intravenous Administration of Linear versus Macrocyclic Gadolinium Chelates. *Radiology, 285*(2), 536-545.

McDonald, R. J., McDonald, J. S., Kallmes, D. F., Jentoft, M. E., Murray, D. L., Thielen, K. R., Williamson, E. E., & Eckel, L. J. (2015). Intracranial Gadolinium Deposition after Contrast-enhanced MR Imaging. *Radiology, 275*(3), 772-782.

McDonald, R. J., McDonald, J. S., Kallmes, D. F., Jentoft, M. E., Paolini, M. A., Murray, D. L., Williamson, E. E., & Eckel, L. J. (2017b). Gadolinium

Deposition in Human Brain Tissues after Contrast-enhanced MR Imaging in Adult Patients without Intracranial Abnormalities. *Radiology, 285*(2), 546-554.

McDonald, W. I., Compston, A., Edan, G., Goodkin, D., Hartung, H. P., Lublin, F. D., McFarland, H. F., Paty, D. W., Polman, C. H., Reingold, S. C., Sandberg-Wollheim, M., Sibley, W., Thompson, A., van den Noort, S., Weinshenker, B. Y., & Wolinsky, J. S. (2001). Recommended diagnostic criteria for multiple sclerosis: guidelines from the International Panel on the diagnosis of multiple sclerosis. *Ann Neurol, 50*(1), 121-127.

Miller, A. E., Wolinsky, J. S., Kappos, L., Comi, G., Freedman, M. S., Olsson, T. P., Bauer, D., Benamor, M., Truffinet, P., O'Connor, P. W., & Group, T. S. (2014). Oral teriflunomide for patients with a first clinical episode suggestive of multiple sclerosis (TOPIC): a randomised, double-blind, placebo-controlled, phase 3 trial. *Lancet Neurol, 13*(10), 977-986.

Miller, D. H., Barkhof, F., & Nauta, J. J. (1993). Gadolinium enhancement increases the sensitivity of MRI in detecting disease activity in multiple sclerosis. *Brain, 116 (Pt 5)*, 1077-1094.

Mohan, J., Krishnaveni, V., & Guo, Y. H. (2014). A survey on the magnetic resonance image denoising methods. *Biomedical Signal Processing and Control, 9*, 56-69.

Montalban, X., Gold, R., Thompson, A. J., Otero-Romero, S., Amato, M. P., Chandraratna, D., Clanet, M., Comi, G., Derfuss, T., Fazekas, F., Hartung, H. P., Havrdova, E., Hemmer, B., Kappos, L., Liblau, R., Lubetzki, C., Marcus, E., Miller, D. H., Olsson, T., Pilling, S., Selmaj, K., Siva, A., Sorensen, P. S., Sormani, M. P., Thalheim, C., Wiendl, H., & Zipp, F. (2018). ECTRIMS/EAN Guideline on the pharmacological treatment of people with multiple sclerosis. *Mult Scler, 24*(2), 96-120.

Muldoon, L. L., & Neuwelt, E. A. (2015). Dose-Dependent Neurotoxicity (Seizures) Due to Deposition of Gadolinium-based Contrast Agents in the Central Nervous System. *Radiology, 277*(3), 925-926.

Multiple Sclerosis International Federation. (2013). Atlas of MS 2013: Mapping Multiple Scerosis around the World. .

Mumford, C. J., Wood, N. W., Kellar-Wood, H., Thorpe, J. W., Miller, D. H., & Compston, D. A. S. (1994). The British Isles survey of multiple sclerosis in twins. *Neurology, 44*(1), 11-11.

Murata, N., Gonzalez-Cuyar, L. F., Murata, K., Fligner, C., Dills, R., Hippe, D., & Maravilla, K. R. (2016). Macrocyclic and Other Non-Group 1 Gadolinium Contrast Agents Deposit Low Levels of Gadolinium in Brain and Bone Tissue:

Preliminary Results From 9 Patients With Normal Renal Function. *Invest Radiol, 51*(7), 447-453.

Neema, M., Stankiewicz, J., Arora, A., Guss, Z. D., & Bakshi, R. (2007). MRI in multiple sclerosis: what's inside the toolbox? *Neurotherapeutics, 4*(4), 602-617.

Patzig, M., Burke, M., Bruckmann, H., & Fesl, G. (2014). Comparison of 3D cube FLAIR with 2D FLAIR for multiple sclerosis imaging at 3 Tesla. *Rofo, 186*(5), 484-488.

Pearce, J. M. (2005). Historical descriptions of multiple sclerosis. *Eur Neurol, 54*(1), 49-53.

Peng, Y., Li, S., Zhuang, Y., Liu, X., Wu, L., Gong, H., Liu, D., & Zhou, F. (2016). Density abnormalities in normal-appearing gray matter in the middle-aged brain with white matter hyperintense lesions: a DARTEL-enhanced voxel-based morphometry study. *Clin Interv Aging, 11*, 615-622.

Polman, C. H., Reingold, S. C., Banwell, B., Clanet, M., Cohen, J. A., Filippi, M., Fujihara, K., Havrdova, E., Hutchinson, M., Kappos, L., Lublin, F. D., Montalban, X., O'Connor, P., Sandberg-Wollheim, M., Thompson, A. J., Waubant, E., Weinshenker, B., & Wolinsky, J. S. (2011). Diagnostic criteria for multiple sclerosis: 2010 revisions to the McDonald criteria. *Ann Neurol, 69*(2), 292-302.

Polman, C. H., Reingold, S. C., Edan, G., Filippi, M., Hartung, H.-P., Kappos, L., Lublin, F. D., Metz, L. M., McFarland, H. F., O'Connor, P. W., M., S.-W., Thompson, A. J., Weinshenker, B. G., & Wolinsky, J. S. (2005). Diagnostic Criteria for Multiple Sclerosis: 2005 Revisions to the "McDonald Criteria". *Annals of Neurology, 58*(6), 840-846.

Port, M., Idee, J. M., Medina, C., Robic, C., Sabatou, M., & Corot, C. (2008). Efficiency, thermodynamic and kinetic stability of marketed gadolinium chelates and their possible clinical consequences: a critical review. *Biometals, 21*(4), 469-490.

Poser, C. M., & Brinar, V. V. (2004). Diagnostic criteria for multiple sclerosis: an historical review. *Clin Neurol Neurosurg, 106*(3), 147-158.

Poser, C. M., Paty, D. W., Scheinberg, L., McDonald, I. W., Davis, F. A., Ebers, G. C., Johnson, K. P., Sibley, W. A., Silberberg, D. H., & Tourtellotte, W. W. (1983). New diagnostic criteria for multiple sclerosis: guidelines for research protocols.

Prins, N. D., & Scheltens, P. (2015). White matter hyperintensities, cognitive impairment and dementia: an update. *Nat Rev Neurol, 11*(3), 157-165.

Pugliatti, M., Rosati, G., Carton, H., Riise, T., Drulovic, J., Vecsei, L., & Milanov, I. (2006). The epidemiology of multiple sclerosis in Europe. *Eur J Neurol, 13*(7), 700-722.

Radbruch, A. (2018). Gadolinium Deposition in the Brain: We Need to Differentiate between Chelated and Dechelated Gadolinium. *Radiology, 288*(2), 434-435.

Radbruch, A., Haase, R., Kieslich, P. J., Weberling, L. D., Kickingereder, P., Wick, W., Schlemmer, H. P., & Bendszus, M. (2017). No Signal Intensity Increase in the Dentate Nucleus on Unenhanced T1-weighted MR Images after More than 20 Serial Injections of Macrocyclic Gadolinium-based Contrast Agents. *Radiology, 282*(3), 699-707.

Radbruch, A., Weberling, L. D., Kieslich, P. J., Eidel, O., Burth, S., Kickingereder, P., Heiland, S., Wick, W., Schlemmer, H. P., & Bendszus, M. (2015). Gadolinium retention in the dentate nucleus and globus pallidus is dependent on the class of contrast agent. *Radiology, 275*(3), 783-791.

Radbruch, A., Weberling, L. D., Kieslich, P. J., Hepp, J., Kickingereder, P., Wick, W., Schlemmer, H. P., & Bendszus, M. (2016). Intraindividual Analysis of Signal Intensity Changes in the Dentate Nucleus After Consecutive Serial Applications of Linear and Macrocyclic Gadolinium-Based Contrast Agents. *Invest Radiol, 51*(11), 683-690.

Radiological Society of North America. (2018). RSNA Statement on Gadolinium-Based MR Contrast Agents.

Rae-Grant, A., Day, G. S., Marrie, R. A., Rabinstein, A., Cree, B. A. C., Gronseth, G. S., Haboubi, M., Halper, J., Hosey, J. P., Jones, D. E., Lisak, R., Pelletier, D., Potrebic, S., Sitcov, C., Sommers, R., Stachowiak, J., Getchius, T. S. D., Merillat, S. A., & Pringsheim, T. (2018). Practice guideline recommendations summary: Disease-modifying therapies for adults with multiple sclerosis: Report of the Guideline Development, Dissemination, and Implementation Subcommittee of the American Academy of Neurology. *Neurology, 90*(17), 777-788.

Reich, D. S., Lucchinetti, C. F., & Calabresi, P. A. (2018). Multiple Sclerosis. *N Engl J Med, 378*(2), 169-180.

Robert, P., Fingerhut, S., Factor, C., Vives, V., Letien, J., Sperling, M., Rasschaert, M., Santus, R., Ballet, S., Idee, J. M., Corot, C., & Karst, U. (2018). One-year Retention of Gadolinium in the Brain: Comparison of Gadodiamide and Gadoterate Meglumine in a Rodent Model. *Radiology, 288*(2), 424-433.

Robert, P., Lehericy, S., Grand, S., Violas, X., Fretellier, N., Idee, J. M., Ballet, S., & Corot, C. (2015). T1-Weighted Hypersignal in the Deep Cerebellar Nuclei After Repeated Administrations of Gadolinium-Based Contrast Agents in Healthy Rats: Difference Between Linear and Macrocyclic Agents. *Invest Radiol, 50*(8), 473-480.

Rocca, M. A., Battaglini, M., Benedict, R. H., De Stefano, N., Geurts, J. J., Henry, R. G., Horsfield, M. A., Jenkinson, M., Pagani, E., & Filippi, M. (2017). Brain MRI atrophy quantification in MS: From methods to clinical application. *Neurology, 88*(4), 403-413.

Roccatagliata, L., Vuolo, L., Bonzano, L., Pichiecchio, A., & Mancardi, G. L. (2009). Multiple sclerosis: hyperintense dentate nucleus on unenhanced T1-weighted MR images is associated with the secondary progressive subtype. *Radiology, 251*(2), 503-510.

Rolf, L., Muris, A. H., Hupperts, R., & Damoiseaux, J. (2016). Illuminating vitamin D effects on B cells--the multiple sclerosis perspective. *Immunology, 147*(3), 275-284.

Roman-Goldstein, S. M., Barnett, P. A., McCormick, C. I., Ball, M. J., Ramsey, F., & Neuwelt, E. A. (1991). Effects of gadopentetate dimeglumine administration after osmotic blood-brain barrier disruption: toxicity and MR imaging findings. *AJNR Am J Neuroradiol, 12*(5), 885-890.

Rossi Espagnet, M. C., Bernardi, B., Pasquini, L., Figa-Talamanca, L., Toma, P., & Napolitano, A. (2017). Signal intensity at unenhanced T1-weighted magnetic resonance in the globus pallidus and dentate nucleus after serial administrations of a macrocyclic gadolinium-based contrast agent in children. *Pediatr Radiol, 47*(10), 1345-1352.

Sastre-Garriga, J., Pareto, D., Battaglini, M., Rocca, M. A., Ciccarelli, O., Enzinger, C., Wuerfel, J., Sormani, M. P., Barkhof, F., Yousry, T. A., De Stefano, N., Tintore, M., Filippi, M., Gasperini, C., Kappos, L., Rio, J., Frederiksen, J., Palace, J., Vrenken, H., Montalban, X., Rovira, A., & group, M. s. (2020). MAGNIMS consensus recommendations on the use of brain and spinal cord atrophy measures in clinical practice. *Nat Rev Neurol, 16*(3), 171-182.

Sawcer, S., Franklin, R. J., & Ban, M. (2014). Multiple sclerosis genetics. *Lancet Neurol, 13*(7), 700-709.

Scalfari, A., Knappertz, V., Cutter, G., Goodin, D. S., Ashton, R., & Ebers, G. C. (2013). Mortality in patients with multiple sclerosis. *Neurology, 81*(2), 184-192.

Schild, H. H. (2012). Contrast media. In *MRI made easy* (pp. 72-75). Berlin: Bayer Pharma AG.

Schlemm, L., Chien, C., Bellmann-Strobl, J., Dorr, J., Wuerfel, J., Brandt, A. U., Paul, F., & Scheel, M. (2017). Gadopentetate but not gadobutrol accumulates in the dentate nucleus of multiple sclerosis patients. *Mult Scler, 23*(7), 963-972.

Schmidt, P., Gaser, C., Arsic, M., Buck, D., Forschler, A., Berthele, A., Hoshi, M., Ilg, R., Schmid, V. J., Zimmer, C., Hemmer, B., & Muhlau, M. (2012). An automated tool for detection of FLAIR-hyperintense white-matter lesions in Multiple Sclerosis. *NeuroImage, 59*(4), 3774-3783.

Sdika, M., & Pelletier, D. (2009). Nonrigid registration of multiple sclerosis brain images using lesion inpainting for morphometry or lesion mapping. *Hum Brain Mapp, 30*(4), 1060-1067.

Smith, A. P., Marino, M., Roberts, J., Crowder, J. M., Castle, J., Lowery, L., Morton, C., Hibberd, M. G., & Evans, P. M. (2017). Clearance of Gadolinium from the Brain with No Pathologic Effect after Repeated Administration of Gadodiamide in Healthy Rats: An Analytical and Histologic Study. *Radiology, 282*(3), 743-751.

Solomon, A. J., & Corboy, J. R. (2017). The tension between early diagnosis and misdiagnosis of multiple sclerosis. *Nat Rev Neurol, 13*(9), 567-572.

Sormani, M. P., & Bruzzi, P. (2013). MRI lesions as a surrogate for relapses in multiple sclerosis: a meta-analysis of randomised trials. *Lancet Neurology, 12*(7), 669-676.

Stojanov, D. A., Aracki-Trenkic, A., Vojinovic, S., Benedeto-Stojanov, D., & Ljubisavljevic, S. (2016). Increasing signal intensity within the dentate nucleus and globus pallidus on unenhanced T1W magnetic resonance images in patients with relapsing-remitting multiple sclerosis: correlation with cumulative dose of a macrocyclic gadolinium-based contrast agent, gadobutrol. *Eur Radiol, 26*(3), 807-815.

Swanton, J. K., Rovira, A., Tintore, M., Altmann, D. R., Barkhof, F., Filippi, M., Huerga, E., Miszkiel, K. A., Plant, G. T., Polman, C., Rovaris, M., Thompson, A. J., Montalban, X., & Miller, D. H. (2007). MRI criteria for multiple sclerosis in patients presenting with clinically isolated syndromes: a multicentre retrospective study. *Lancet Neurol, 6*(8), 677-686.

Thompson, A., Banwell, B. L., Barkhof, F., Carroll, W. M., Coetzee, T., Comi, G., Correale, J., Fazekas, F., Filippi, M., Freedman, M. S., Fujihara, K., Galetta, S. L., Hartung, H. P., Kappos, L., Lublin, F. D., Marrie, R. A., Miller, A. E., Miller, D. H., Montalban, X. r., Mowry, E. M., Sorensen, P. S., Tintoré, M., Traboulsee, A. L., Trojano, M., Uitdehaag, B. M. J., Vukusic, S., Waubant, E., Weinshenker, B. G., Reingold, S. C., & Cohen, J. A. (2015). Functional brain

networks: linking thalamic atrophy to clinical disability in multiple sclerosis, a multimodal fMRI and MEG study. *Hum Brain Mapp, 36*(2), 603-618.

Thompson, A., Baranzini, S. E., Geurts, J., Hemmer, B., & Ciccarelli, O. (2018a). Multiple sclerosis. *The Lancet, 391*(10130), 1622-1636.

Thompson, A. J., Banwell, B. L., Barkhof, F., Carroll, W. M., Coetzee, T., Comi, G., Correale, J., Fazekas, F., Filippi, M., Freedman, M. S., Fujihara, K., Galetta, S. L., Hartung, H. P., Kappos, L., Lublin, F. D., Marrie, R. A., Miller, A. E., Miller, D. H., Montalban, X., Mowry, E. M., Sorensen, P. S., Tintore, M., Traboulsee, A. L., Trojano, M., Uitdehaag, B. M. J., Vukusic, S., Waubant, E., Weinshenker, B. G., Reingold, S. C., & Cohen, J. A. (2018b). Diagnosis of multiple sclerosis: 2017 revisions of the McDonald criteria. *Lancet Neurol, 17*(2), 162-173.

Traboulsee, A., Simon, J. H., Stone, L., Fisher, E., Jones, D. E., Malhotra, A., Newsome, S. D., Oh, J., Reich, D. S., Richert, N., Rammohan, K., Khan, O., Radue, E. W., Ford, C., Halper, J., & Li, D. (2016). Revised Recommendations of the Consortium of MS Centers Task Force for a Standardized MRI Protocol and Clinical Guidelines for the Diagnosis and Follow-Up of Multiple Sclerosis. *AJNR Am J Neuroradiol, 37*(3), 394-401.

U.S. Food and Drug Administration, F. (2015). Drug Safety Communications: FDA evaluating the risk of brain deposits with repeated use of gadolinium-based contrast agents for magnetic resonance imaging (MRI).

Valsasina, P., Aboulwafa, M., Preziosa, P., Messina, R., Falini, A., Comi, G., Filippi, M., & Rocca, M. A. (2018). Cervical Cord T1-weighted Hypointense Lesions at MR Imaging in Multiple Sclerosis: Relationship to Cord Atrophy and Disability. *Radiology, 288*(1), 234-244.

Valverde, S., Oliver, A., & Llado, X. (2014). A white matter lesion-filling approach to improve brain tissue volume measurements. *Neuroimage Clin, 6*, 86-92.

Van Leemput, K., Maes, F., Vandermeulen, D., & Suetens, P. (1999). Automated model-based bias field correction of MR images of the brain. *IEEE Transactions on Medical Imaging, 18*(10), 885-896.

Vercellino, M., Masera, S., Lorenzatti, M., Condello, C., Merola, A., Mattioda, A., Tribolo, A., Capello, E., Mancardi, G. L., Mutani, R., Giordana, M. T., & Cavalla, P. (2009). Demyelination, inflammation, and neurodegeneration in multiple sclerosis deep gray matter. *J Neuropathol Exp Neurol, 68*(5), 489-502.

Vrenken, H., Jenkinson, M., Horsfield, M. A., Battaglini, M., van Schijndel, R. A., Rostrup, E., Geurts, J. J., Fisher, E., Zijdenbos, A., Ashburner, J., Miller, D. H., Filippi, M., Fazekas, F., Rovaris, M., Rovira, A., Barkhof, F., de Stefano, N., &

Group, M. S. (2013). Recommendations to improve imaging and analysis of brain lesion load and atrophy in longitudinal studies of multiple sclerosis. *J Neurol, 260*(10), 2458-2471.

Wattjes, M. P., Lutterbey, G. G., Harzheim, M., Gieseke, J., Traber, F., Klotz, L., Klockgether, T., & Schild, H. H. (2006). Imaging of inflammatory lesions at 3.0 Tesla in patients with clinically isolated syndromes suggestive of multiple sclerosis: a comparison of fluid-attenuated inversion recovery with T2 turbo spin-echo. *Eur Radiol, 16*(7), 1494-1500.

Weberling, L. D., Kieslich, P. J., Kickingereder, P., Wick, W., Bendszus, M., Schlemmer, H. P., & Radbruch, A. (2015). Increased Signal Intensity in the Dentate Nucleus on Unenhanced T1-Weighted Images After Gadobenate Dimeglumine Administration. *Invest Radiol, 50*(11), 743-748.

Weishaupt, D., Köchli, V. D., & Marincek, B. (2006a). *How does MRI work?* Berlin Heidelberg: Springer-Verlag.

Weishaupt, D., Köchli, V. D., & Marincek, B. (2006b). MR contrast agents. In *How does MRI work? - An Introduction to the Physics and Function of Magnetic Resonance Imaging* (pp. 103-128). Berlin Heidelberg: Springer-Verlag.

Willer, C. J., Dyment, D. A., Risch, N. J., Sadovnick, A. D., Ebers, G. C., & Canadian Collaborative Study, G. (2003). Twin concordance and sibling recurrence rates in multiple sclerosis. *Proc Natl Acad Sci U S A, 100*(22), 12877-12882.

Young, I. R., Hall, A. S., Pallis, C. A., Legg, N. J., Bydder, G. M., & R.E., S. (1981). Nuclear magnetic resonance imaging of the brain in multiple sclerosis. *Lancet, 2*, 1063-1066.

Young, L. K., Matthew, S. Z., & Houston, J. G. (2019). Absence of potential gadolinium toxicity symptoms following 22,897 gadoteric acid (Dotarem®) examinations, including 3,209 performed on renally insufficient individuals. *Eur Radiol, 29*(4), 1922-1930.

Zijdenbos, A. P., Forghani, R., & Evans, A. C. (2002). Automatic "pipeline" analysis of 3-D MRI data for clinical trials: application to multiple sclerosis. *IEEE Trans Med Imaging, 21*(10), 1280-1291.

Zivadinov, R., Bergsland, N., Hagemeier, J., Ramasamy, D. P., Dwyer, M. G., Schweser, F., Kolb, C., Weinstock-Guttman, B., & Hojnacki, D. (2019). Cumulative gadodiamide administration leads to brain gadolinium deposition in early MS. *Neurology, 93*(6), e611-e623.

7 Publications

Grahl, S., Bussas, M., Pongratz, V., Kirschke, J. S., Zimmer, C., Berthele, A., Hemmer, B., & Muehlau, M. (2020). T1-Weighted Intensity Increase After a Single Administration of a Linear Gadolinium-Based Contrast Agent in Multiple Sclerosis. *Clin Neuroradiol*. doi:10.1007/s00062-020-00882-6

Engl, C., Tiemann, L., **Grahl, S.**, Bussas, M., Schmidt, P., Pongratz, V., Berthele, A., Beer, A., Gaser, C., Kirschke, J. S., Zimmer, C., Hemmer, B., & Muehlau, M. (2020). Cognitive impairment in early MS: contribution of white matter lesions, deep grey matter atrophy, and cortical atrophy. *J Neurol*. doi:10.1007/s00415-020-09841-0

Grahl, S., Pongratz, V., Schmidt, P., Engl, C., Bussas, M., Radetz, A., Gonzalez-Escamilla, G., Groppa, S., Zipp, F., Lukas, C., Kirschke, J., Zimmer, C., Hoshi, M., Berthele, A., Hemmer, B., & Muehlau, M. (2019). Evidence for a white matter lesion size threshold to support the diagnosis of relapsing remitting multiple sclerosis. *Mult Scler Relat Disord, 29,* 124-129. doi:10.1016/j.msard.2019.01.042

Grahl, S., Bussas, M., Pongratz, V., Gasperi, C., Berthele, A., Kirschke, J., Zimmer, C., Hemmer, B., Muehlau, M. (2019). Determinants of cognitive screening tests for MS patients. Poster at European Committee for Treatment and Research in Multiple Sclerosis Conference- ECTRIMS.

Pongratz, V., Schmidt, P., Bussas, M., **Grahl, S.**, Gaser, C., Berthele, A., Hoshi, M. M., Kirschke, J., Zimmer, C., Hemmer, B. & Muehlau, M. (2019). Prognostic value of white matter lesion shrinking in early multiple sclerosis: An intuitive or naïve notion? *Brain and Behavior, 9(12),* e01417.

Wuschek, A., **Grahl, S.**, Pongratz, V., Korn, T., Kirschke, J., Zimmer, C., Hemmer, B., & Muehlau, M. (2019). CSF protein concentration shows no correlation with brain volume measures. *Frontiers in Neurology, 10*, 463.

Grahl, S., Bussas, M., Gasperi, C., Pongratz, V., Hoshi, MM., Berthele, A., Kirschke, J., Zimmer, C., Hemmer, B., Muehlau, M. (2018). T1-weighted signal intensity change in the dentate nucleus of MS patients after repeated application of linear and macrocyclic gadolinium-based contrast agents. Presentation at European Committee for Treatment and Research in Multiple Sclerosis Conference - ECTRIMS.

Grahl, S., Pongratz née Biberacher, V., Schmidt, P., Engl, C., Bussas, M., Radetz, A., Fleischer, V., Zipp, F., Groppa, S., Kirschke, J., Zimmer, C., Hoshi, MM., Berthele, A., Hemmer, B., Muehlau, M. (2017). Defining a Minimal Meaningful Lesion Size in Multiple Sclerosis. Poster at European Committee for Treatment and Research in Multiple Sclerosis Conference - ECTRIMS.

Grahl, S., Biberacher, V., Schmidt, P., Beer, A., Kirschke, J., Zimmer, C., Hemmer, B., Muehlau, M. (2017). Is there a threshold for the minimal meaningful lesion size in multiple sclerosis?. Poster at Fondation ARSEP - French MS Research Society Conference.